OPEN ACCESS
IOP Publishing

Made open access 3 April 2020
Classical and Quantum Gravity

Class. Quantum Grav. **36** (2019) 205007 (43pp) https://doi.org/10.1088/1361-6382/ab3523

Rotation of polarization in the gravitational field of a laser beam—Faraday effect and optical activity

Fabienne Schneiter[1], **Dennis Rätzel**[2,3] **and Daniel Braun**[1]

[1] Eberhard-Karls-Universität Tübingen, Institut für Theoretische Physik, 72076 Tübingen, Germany
[2] Institut für Physik, Humboldt-Universität zu Berlin, Newtonstraße 15, 12489 Berlin, Germany

E-mail: dennis.raetzel@physik.hu-berlin.de

Received 28 February 2019, revised 12 July 2019
Accepted for publication 22 July 2019
Published 18 September 2019

Abstract

We investigate the rotation of the polarization of a light ray propagating in the gravitational field of a circularly polarized laser beam. The rotation consists of a reciprocal part due to gravitational optical activity, and a non-reciprocal part due to the gravitational Faraday effect. We discuss how to distinguish the two effects: letting light propagate back and forth between two mirrors, the rotation due to gravitational optical activity cancels while the rotation due to the gravitational Faraday effect accumulates. In contrast, the rotation due to both effects accumulates in a ring cavity and a situation can be created in which gravitational optical activity dominates. Such setups amplify the effects by up to five orders of magnitude, which however is not enough to make them measurable with state of the art technology. The effects are of conceptual interest as they reveal gravitational spin–spin coupling in the realm of classical general relativity, a phenomenon which occurs in perturbative quantum gravity.

Keywords: linearized gravity, spin angular momentum of light, spin–spin coupling of light, gravitational Faraday effect, gravitational optical activity, general relativity, gravity of light

(Some figures may appear in colour only in the online journal)

[3] Author to whom any correspondence should be addressed.

 © 2019 IOP Publishing Ltd Printed in the UK

This is an open access article distributed under the terms of the Creative Commons Attribution 4.0 License.
Any further distribution of this work must maintain attribution to the author(s) and the title of the work, journal citation and DOI.

1. Introduction

The gravitational field of a light beam was first studied in 1931 by Tolman, Ehrenfest and Podolski [1], who described a light beam in the simplest way, namely as a single light ray of constant energy density and without polarization. Since then, various models for light beams have been considered, such as in [2–4], all of them having in common that the short-wavelength approximation is used. This means that the light is either described as a thin pencil or as a continuous fluid moving at the speed of light and without any wave-like properties. Recently, we studied the gravitational field of a laser beam beyond the short-wavelength approximation [5]: the laser beam is modeled as a solution of Maxwell's equations, and therefore, has wave-like properties. In this case, there appear gravitational effects of light that were not visible in the previous models, such as frame-dragging due to the light's spin angular-momentum, the deflection of a parallel propagating test ray, and the rotation of polarization of test rays. The latter is the subject of this article.

Effects of gravitational rotation of polarization were first described in 1957 independently by Skrotsky [6] and by Balazs [7]. In 1960, Plebanski found a coordinate-invariant expression for the change of the polarization for a light ray coming from flat spacetime, passing through a weak gravitational field, and going to flat spacetime again [8]. The gravitational rotation of polarization has been studied for several systems: for moving objects, moving gravitational lenses [9–11] and other astrophysical situations [12, 13], in the context of gravitational waves [14], for rotating rings [15], for ring lasers [16] and for linearly polarized lasers in a waveguide [17]. It was also treated more formally in [18–20].

Rotation of polarization is well-known from classical optics, when light rays pass through certain media (see e.g. [21]). For this, the medium needs broken inversion symmetry, a property certain materials have naturally. Such media with 'natural optical activity' lead to different phase velocities of right- and left-circularly polarized light. The effect is 'reciprocal', i.e. when the light ray is reflected back through the medium, the rotation of polarization is undone. In contrast hereto is the Faraday effect, which can be created even in isotropic media by applying a magnetic field. Here, the rotation is 'non-reciprocal', i.e. the polarization keeps rotating in the same direction relative to the original frame when the light propagates back along the path. In this article, we consider the rotation of the polarization vector of test rays in the gravitational field of a circularly polarized laser beam in free space. It turns out that the rotation of polarization contains both a reciprocal and a non-reciprocal part. The former can hence be interpreted as gravitational optical activity and the latter as a gravitational Faraday effect, also called Skrotsky effect.

The laser beam is described as a perturbative solution to Maxwell's equations, an expansion in the beam divergence angle θ, which is assumed to be smaller than one radian. The description of the laser beam and its gravitational field is given in detail in [5] and summarized below. We look at the rotation of the polarization of test rays which are parallel co-propagating, parallel counter-propagating, or propagating transversally to the beamline of the source laser-beam, and consider a cavity where the rotation of the polarization vector accumulates after each roundtrip. We thus propose a measurement scheme which may possibly be realized in a laboratory in the future, when the sensitivity in experiments has improved accordingly.

The description of the gravitational field of a laser beam is reviewed in section 2, and the calculation of the rotation of light polarization in curved spacetime in section 3. In section 4, we calculate the Faraday effect for test rays. As already mentioned, only the non-reciprocal part of the rotation which is not due to the deflection can be associated with the Faraday effect, which is discussed in section 5. Considering a cavity in a certain arrangement, the rotation angles acquired after each roundtrip of the light inside the cavity sum up. This is the subject of section 6, where we look at a one-dimensional cavity and a ring cavity and discuss the possible measurement precision of the rotation angle. We give a conclusion and an outlook in section 7.

To keep track of the orders of magnitude, we introduce dimensionless coordinates by dividing them by the beam waist w_0 as $\tau = ct/w_0$, $\xi = x/w_0$, $\chi = y/w_0$ and $\zeta = z/w_0$, where c is the speed of light. Greek indices like x^α refer to dimensionless spacetime coordinates and latin indices like x^a refer to dimensionless spatial coordinates. For the spacetime metric, we choose the sign convention $(-,+,+,+)$, such that the Minkowski metric η in the dimensionless coordinates reads $\eta = w_0^2 \mathrm{diag}(-1,1,1,1)$. In the numerical examples and plots, we use the following values: the beam waist $w_0 = 10^{-6}$ m, the beam divergence $\theta = 0.3$ rad (this determines the wavelength, which is given by $\pi\theta w_0 \simeq 1$ μm), the polarization $\lambda = 1$, and the power of the source laser-beam, which is directed in the positive z-direction, $P_0 = 10^{15}$ W.

2. The gravitational field of a laser beam beyond the short wavelength approximation

In this section, we summarize the description of the laser beam and its gravitational field presented in [5]. A laser beam is accurately described by a Gaussian beam. The Gaussian beam is a monochromatic electromagnetic, almost plane wave whose intensity distribution decays with a Gaussian factor with the distance to the beamline. It is obtained as a perturbative solution of Maxwell's equations, namely an expansion in the beam divergence θ, the opening angle of the beam, which is assumed to be smaller than one radian. The electromagnetic four-vector potential describing the Gaussian beam is obtained by a plane wave multiplied by an envelope function that is assumed to vary slowly in the direction of propagation, in agreement with the property that the divergence of the beam is small. Corresponding to these features, one makes the ansatz for the four-vector potential $A_\alpha(\tau,\xi,\chi,\zeta) = \tilde{\mathcal{A}} v_\alpha(\xi,\chi,\theta\zeta)\mathrm{e}^{\mathrm{i}\frac{2}{\theta}(\zeta-\tau)}$, where $\tilde{\mathcal{A}}$ is the amplitude and v_α the envelope function[4]. The exponential factor describes a plane wave propagating in ζ-direction with wave number $k = 2/(\theta w_0)$, where w_0 is the beam waist at its focal point. The laser beam propagates in positive ζ-direction such that its beamline concides with the ζ-axis. The beam is illustrated in figure 1.

Like the four-vector potential for any radiation, A_α satisfies the Maxwell equations, which, in vacuum, are given by the wave equations

$$\left(-\partial_\tau^2 + \partial_\xi^2 + \partial_\chi^2 + \partial_\zeta^2\right) A_\alpha(\tau,\xi,\chi,\zeta) = 0, \tag{1}$$

where the Lorenz-gauge condition is chosen. Since the envelope function varies slowly in the direction of propagation, the wave equations (1) reduce to a Helmholtz equation for each component of the envelope function,

$$\left(\partial_\xi^2 + \partial_\chi^2 + \theta^2\partial_{\theta\zeta}^2 + 4iw_0\partial_{\theta\zeta}\right) v_\alpha(\xi,\chi,\theta\zeta) = 0. \tag{2}$$

This Helmholtz equation is solved by writing the envelope function as a power series in the small parameter θ. One obtains an equation for each order of the expansion of the envelope function, with a source term consisting of the solution for a lower order, where even and odd orders do not mix. The beam is assumed to have left- or right-handed circular polarization, which we label by $\lambda = \pm 1$[5]. We define this to be the case if its field strength, defined as $F_{\alpha\beta} = \partial_\alpha A_\beta - \partial_\beta A_\alpha$, is an eigenfunction with eigenvalue ± 1 of the generator of the duality

[4] More precisely, the complex-valued vector potential A we consider is the analytical signal of the real-valued physical vector potential, which is obtained by taking the real part of A.

[5] The vector potential describing the laser beam thus depends on the parameter λ, and so do its energy-momentum tensor, the induced metric perturbation and the effects we calculate in the following sections. Therefore, these quantities can be thought of as being labelled by an index λ, which we suppress in the following, except for appendix A, where we write the index λ explicitly.

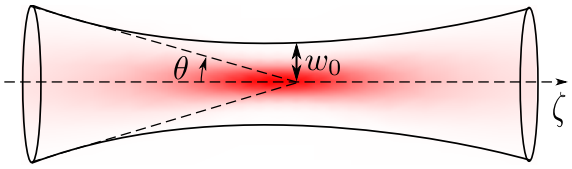

Figure 1. Schematic illustration of the laser beam propagating in the positive ζ-direction: the beam divergence θ describes the opening angle of the laser beam and is assumed to be a small parameter (smaller than 1 rad), and the beam waist w_0 is a measure for the radius of the laser beam at its focal point. The intensity of the laser beam decreases with a Gaussian factor with the distance from the beamline.

transformation of the electromagnetic field given by $F_{\alpha\beta} \mapsto -\mathrm{i}\epsilon_{\alpha\beta\gamma\delta}F^{\gamma\delta}/2$, where $\epsilon_{\alpha\beta\gamma\delta}$ is the completely anti-symmetric tensor with $\epsilon_{0123} = -1$. Our definition of helicity is based on the invariance of Maxwell's equations under the duality transformation and the conservation of the difference between photon numbers of right- and left-polarized photons shown in [22] (see also [23–26]). For $\theta = 0$, this leads to the usual expressions for the field strength of a circularly polarized laser beam.

It turns out that the energy-momentum tensor, which one may expect to be oscillating at the frequency of the laser beam, does not contain any oscillating terms when circular polarization is assumed. The energy-momentum tensor reads (see appendix A for the explicit expressions)

$$T_{\alpha\beta} = \frac{c^2\epsilon_0}{2}\,\mathrm{Re}\left(F_\alpha{}^\sigma F^*_{\beta\sigma} - \frac{1}{4}\eta_{\alpha\beta}F^{\delta\rho}F^*_{\delta\rho}\right). \tag{3}$$

The power series expansion of the envelope function induces a power series expansion of the energy-momentum tensor and the expansion coefficients are identified as different order terms of $T_{\alpha\beta}$ in θ.

Since the energy density of a laser beam is small compared to the one of ordinary matter, one may expect its gravitational field to be weak. The spacetime metric describing the gravitational field is thus assumed to consist of the metric for flat spacetime $\eta_{\alpha\beta}$ plus a small perturbation $h_{\alpha\beta}$. Terms quadratic in the metric perturbation are neglected; this is the linearized theory of general relativity. In this case, the Einstein field equations reduce to wave equations for the metric perturbation [27]

$$\frac{1}{w_0^2}\left(-\partial_\tau^2 + \partial_\xi^2 + \partial_\chi^2 + \partial_\zeta^2\right)h_{\alpha\beta} = -\frac{16\pi G}{c^4}T_{\alpha\beta}, \tag{4}$$

where G is Newton's constant and where the Lorenz-gauge has been chosen. Like the envelope function and the energy-momentum tensor, the metric perturbation is expanded in the beam divergence,

$$h_{\alpha\beta}(\xi,\chi,\theta\zeta) = \sum_{n=0}^{\infty}\theta^n h^{(n)}_{\alpha\beta}(\xi,\chi,\theta\zeta). \tag{5}$$

For a laser beam extending from minus to plus spatial infinity, the wave equations (4) result in a two-dimensional Poisson equation for each $h^{(n)}_{\alpha\beta}$, with a source term consisting of a term of the energy-momentum tensor of the same order and a term proportional to $h^{(n-2)}_{\alpha\beta}$, where even and odd orders do not mix. Details and the solutions for the zeroth, the first and the third order, which are relevant for our purposes, are given in appendix A.

For a finitely extended source beam, the solution of (4) with time-independent energy-momentum tensor of the source laser-beam can be calculated using the Green's function of the three-dimensional Poisson equation,

$$h_{\alpha\beta} = \frac{4Gw_0^2}{c^4} \int \mathrm{d}\xi' \mathrm{d}\chi' \mathrm{d}\zeta' \frac{T_{\alpha\beta}\left(\xi', \chi', \theta\zeta'\right)}{|\vec{x} - \vec{x}'|}, \tag{6}$$

where $\vec{x} = (\xi, \chi, \zeta)$ and $\vec{x}' = (\xi', \chi', \zeta')$. The solution (6) is discussed in detail in [5].

3. Rotation of polarization in a weakly curved spacetime

In this section, we explain the expression presented in [8] for the rotation angle that the polarization vector of a test ray acquires when propagating in a gravitational field.

For a light ray propagating through a gravitational field and starting and ending at spatial infinity, the rotation angle of polarization within a plane perpendicular to the propagation direction (in the following called ray-transverse plane) is given by equation (5.33) in [8]. For our set of coordinates, it takes the form

$$\Delta = \frac{1}{2w_0^2} \int_{-\infty}^{\infty} \mathrm{d}\tau \; t_0^a \epsilon_{abc} \partial_b h_{c\alpha}(\tau, \varrho_\perp + \tau t_0) t_0^\alpha, \tag{7}$$

where ϵ_{abc} is the Levi-Civita symbol in three dimensions with $\epsilon_{123} = 1$, $t_0^a = \dot{\gamma}^a(\tau_0)$ is the initial tangent to the curve describing the light ray parametrized by the dimensionless parameter τ, and the line $\varrho_\perp + \tau t_0$ with $\varrho_\perp = (\xi_0, \chi_0, 0)$ constant is equivalent to the spatial part of the ray γ including terms up to linear order in the metric perturbation. Therefore, the evaluation of the metric perturbation along the line $\varrho_\perp + \tau t_0$ instead of γ the actual, possibly deflected trajectory of a light ray in the gravitational field of the source is justified as the correction would be of higher order in the metric perturbation.

The sign of the rotation angle Δ is chosen such that the positive sign refers to right-handedness (handedness of rotation as inferred from equation (5.20) of [8]). Equation (7) was obtained using the formal analogy of Maxwell's equations in a dielectric medium and Maxwell's equations in a gravitational field and using geometric ray optics for vectors. It is shown in [8] that the expression in equation (7) is invariant under coordinate transformations that approach the identity at spatial infinity. For equation (7) to be valid, the metric perturbation and all its first derivatives have to vanish at least as $\tilde{\rho}^{-1}$ for $\tilde{\rho} \to \infty$, where $\tilde{\rho} = \sqrt{\xi^2 + \chi^2 + \zeta^2}$.

For a light ray that is not deflected by the gravitational field, i.e. that does not change its direction of propagation, the ray-transverse plane is the same everywhere far away from the laser beam, where spacetime is flat. However, when the light ray is deflected, this plane is tilted after passing the gravitational field with respect to the one before entering the gravitational field. Therefore, the rotation of the polarization vector within the ray-transverse plane given in equation (7) is superimposed with a change of the polarization vector $\delta\vec{\omega}$ due to the deflection of the light ray. The latter consists of a rotation plus a deformation which depend on the initial polarization vector $\vec{\omega}$[6]. It does not contribute to the gravitational Faraday effect or the optical activity. An experimentalist who wants to measure only optical activity and the gravitational Faraday effect would have to correct for deflection. The change of the polarization vector is illustrated in figure 2.

Another approach to determine the rotation of polarization is described in appendix B. It agrees with the results presented in this section.

For a linearly polarized test ray, the interpretation of the rotation of the polarization vector is clear: for example, for a test light-ray propagating in ζ-direction, the

[6] See section 6 in [8].

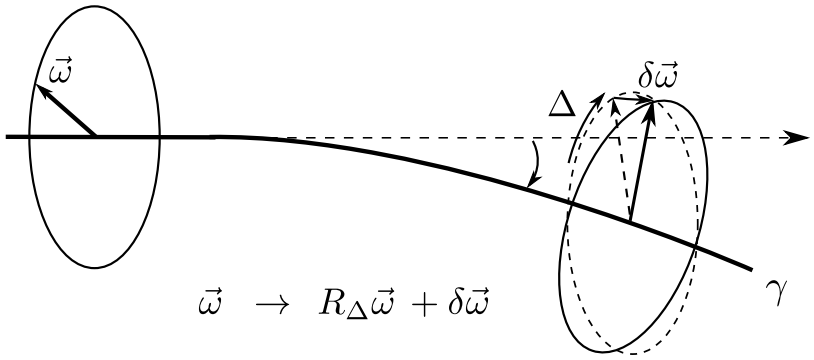

Figure 2. Change of the initial polarization vector $\vec{\omega}$ of a light ray γ: the initial polarization vector $\vec{\omega}$ in the initial ray-transverse plane (represented by the solid circle on the left and the dashed circle on the right) is rotated by the angle Δ into $R_\Delta\vec{\omega}$ (dashed arrow on the right) due to the gravitational field, where R_Δ is the corresponding rotation matrix. Additionally, the deflection of the laser beam tilts the ray-transverse plane into its final orientation (solid circle on the right) such that it stays orthogonal to the tangent of the deflected laser beam. The tilt leads to an additional change $\delta\vec{\omega}$ of the polarization vector $\vec{\omega}$. The rotation by the angle Δ consists of a reciprocal part due to the gravitational optical activity and a non-reciprocal part due to the gravitational Faraday effect.

polarization vector describing linear polarization in ξ-direction, $\vec{\epsilon}_\xi = (1,0,0)$, is rotated into $R_\Delta\vec{\epsilon}_\xi = (\cos(\Delta),\sin(\Delta),0)$, where R_Δ stands for the matrix rotating by the angle Δ about the ζ-axis. For a circularly polarized test ray with helicity $\lambda_{\text{test}} = \pm 1$ and with the corresponding polarization vector $\vec{\epsilon}_{\lambda_{\text{test}}} = (1, -\lambda_{\text{test}}i, 0)/\sqrt{2}$, one obtains $R_\Delta\vec{\epsilon}_{\lambda_{\text{test}}} = \mathrm{e}^{\mathrm{i}\lambda_{\text{test}}\Delta}\vec{\epsilon}_{\lambda_{\text{test}}}$. This means that the circularly polarized test ray acquires the phase $\lambda_{\text{test}}\Delta$. In general, for an elliptically polarized test light ray, the acquired phases of the circular components lead to a rotation of the major axis of the ellipse by an angle Δ.

4. Rotation of polarization in the gravitational field of a laser beam

In this section, we investigate the rotation of the polarization vector of a test ray passing through the gravitational field of a source laser-beam according to equation (7).

We consider different orientations of the test ray with respect to the source beam: parallel co-propagating, parallel counter-propagating, and transversal test rays. We find that the effect depends strongly on the orientation of the test ray. In particular, we obtain that the order of the metric expansion[7] that causes the rotation of polarization depends on the orientation of the test ray.

The source laser-beam is assumed to propagate along the ζ-axis, to be emitted at $\zeta = \alpha$ and absorbed at $\zeta = \beta$. The parallel co-propagating test ray is emitted at $\zeta = A$ and absorbed at $\zeta = B$ and the parallel counter-propagating test ray is emitted at $\zeta = B$ and absorbed at $\zeta = A$. The test ray that is oriented transversally to the beamline of the source laser-beam is emitted at $\xi = A$ and absorbed at $\xi = B$ or vice versa.

In section 4.1 we focus on an ideal situation of infinitely long test rays. The source laser-beam is considered to be either finitely or infinitely extended. In section 4.2 we look at finitely

[7] Generally, with the order of the metric expansion, we refer to the order in θ. Any higher order terms of the metric perturbation itself are neglected in the linearized theory of general relativity.

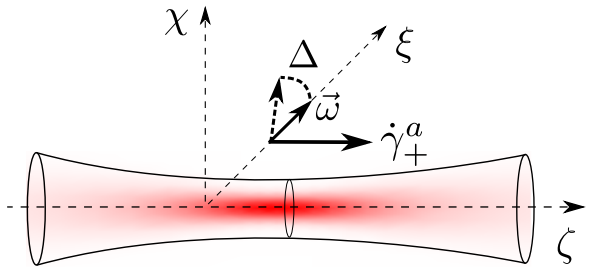

Figure 3. Schematic illustration of the rotation of the polarization vector $\vec{\omega}$ (here it originally has only a component in ξ-direction) of a parallel co-propagating test ray with tangent $\dot{\gamma}_+$ in the gravitational field of the laser beam.

long test rays and a finitely extended source laser-beam, and we discuss the the long-range behavior of the rotation of polarization of the test rays. In section 4.3, we discuss the gravitational coupling between the spin of the source laser-beam and the spin of the test ray.

4.1. Infinitely extended test ray

For the infinitely extended test rays, the conditions for the application of equation (7) are immediately seen to be fulfilled for the finitely extended source beam, as the metric perturbation and all its first derivatives vanish at least as $\tilde{\rho}^{-1}$ for $\tilde{\rho} \to \infty$. This follows directly from the Green's function which is proportional to $1/\tilde{\rho}$ in three dimensions.

For the parallel test rays, for an infinitely extended source beam and an infinitely extended test ray it will always be understood that the emitter and absorber of the test ray are sent to infinity more rapidly than those of the source-beam, i.e. $|A|, |B| \gg |\alpha|, |\beta| \to \infty$, such that also here the test ray indeed begins and ends in flat spacetime. For the transversal test rays, for an infinitely extended source beam and infinitely extended test rays, it is assumed that $|A|$ and $|B|$ approach infinity fast enough for them to be in flat spacetime.

Besides the strict validity of equation (7), the infinite test-ray has also the advantage to lead to relatively simple analytical expressions for the rotation angles.

4.1.1. Parallel test rays. We start by looking at the rotation of the polarization vector of test rays which are parallel co-propagating or counter-propagating with respect to the source laser-beam as illustrated in figure 3.

The parallel co- and counter-propagating test rays are assumed to have a distance $\rho = \sqrt{\xi^2 + \chi^2}$ from the beamline, and to travel from $\zeta = -\infty$ to $\zeta = \infty$ and from $\zeta = \infty$ to $\zeta = -\infty$, respectively. They are considered to have transversal polarization described by the polarization vector $w^\mu = (0, w^\xi, w^\chi, 0)$. The initial tangents to their worldlines are given by $\dot{\gamma}_\pm(\tau_0) = (1, 0, 0, \pm(1 - f^\pm))$, where the '+' corresponds to the co-propagating test ray and the ' − ' to the counter-propagating test ray. The parameter $f^\pm$ ensures that $\dot{\gamma}_\pm$ satisfies the null condition. It is proportional to the metric perturbation, which means that it does not contribute in equation (7) and can be neglected in the following calculations. Since the integration in equation (7) is along the line $\varrho_\perp + \tau t_0 = (\xi_0, \chi_0, \pm\tau)$, we can change the integration variable from τ to ζ when neglecting terms quadratic in the metric perturbation. Then, for the parallel propagating test rays we obtain (see equation (D.1))

$$\Delta_\pm = -\frac{1}{2w_0^2} \int_{-\infty}^{\infty} \mathrm{d}\zeta \Big(\partial_\chi \left(h_{\xi\zeta} \pm h_{\tau\xi} \right) - \partial_\xi \left(h_{\chi\zeta} \pm h_{\tau\chi} \right) \Big). \tag{8}$$

Notice that the metric perturbation contains a factor w_0^2, such that $\Delta_\pm$ is dimensionless. For the co-propagating test ray, the contribution coming from the first order of the metric perturbation cancels, and one obtains in leading order (the third order in θ)

$$\Delta_+ = \lambda \frac{GP_0\theta^3}{c^5} \int_\alpha^\beta \mathrm{d}\zeta\, |\mu|^2(1+2|\mu|^2\rho^2)\mathrm{e}^{-2|\mu|^2\rho^2}, \tag{9}$$

where $|\mu|^2 = (1+(\theta\zeta)^2)^{-1}$. Note that ζ in (9) parametrizes the source beam (i.e. corresponds to ζ' in (6)). The derivation of (9) (see appendix E for details) uses an asymptotic expansion in $1/B$, i.e. assumes that $B \gg |\zeta'|, |\rho'|$, as well as a finite cut-off ρ_0 of the energy density in radial direction that is then sent to infinity. The expression with ρ_0 kept finite is given by (E.15). For an infinitely extended source beam, we can then simply evaluate the limit $\alpha \to -\infty$ and $\beta \to \infty$. An alternative derivation that starts from an infinitely extended source beam and an infinitely extended test ray is given in appendix D.

The integrand in (9) decreases as a Gaussian with the distance to the beamline. The Gaussian factor is the same as the one that appears as a global factor in the energy-momentum tensor of the source beam (see [5] or appendix A), which implies that significant contributions to Δ_+ for the infinitely extended test ray are only accumulated in regions where the energy distribution of the source beam does not vanish. In addition, (E.15) shows that there is no effect outside of a finite beam when a cut-off of the energy-momentum distribution is considered.

The sign of the rotation angle in equation (9) depends on λ, which specifies the handedness of the light in the source laser-beam. The dependence of the rotation angle Δ_+ on the distance to the beamline is illustrated in the upper graph of figure 4.

For the counter-propagating test ray, we obtain in leading order (the first order in θ)

$$\Delta_- = -\lambda \frac{8GP_0\theta}{c^5} \int_\alpha^\beta \mathrm{d}\zeta\, |\mu|^2 \mathrm{e}^{-2|\mu|^2\rho^2} \tag{10}$$

for the finitely extended source beam and the infinitely extended test ray. Equation (10) is derived with the same limiting procedures as (9). Its version with finite radial cut-off of $T_{\mu\nu}$ is given in (E.8). The integrand in equation (10) decreases in the same way as the one in equation (9) with the same Gaussian factor with the distance to the beamline that can be found as a global factor in the energy-momentum tensor of the laser beam. We find that there are no significant contributions to the rotation angle Δ_- outside of the energy distribution for an infinitely extended test ray (see equation (E.8)) when introducing a cut-off of the energy-momentum distribution in transversal direction. The dependence of the rotation angle Δ_- on the distance to the beamline is illustrated in the lower graph in figure 4. The two orders of magnitude larger values for Δ_- compared to those for Δ_+ arise due to the factor $\theta^2/8$ present in the expression for Δ_+ but not in the one for Δ_- (compare equations (9) and (10)).

4.1.2. Transversally propagating test rays. The transversally propagating test ray is described by the initial tangent $\dot\gamma_\pm = (1, \pm(1-f^\pm), 0, 0)$. Due to the same argument as before, we do not have to take into account the parameter $f^\pm$. For the rotation angle of the polarization vector, we obtain for the infinitely extended source beam and infinitely extended test ray (see appendix D for the detailed derivation) including terms up to first order

$$\begin{aligned}\Delta_{\mathrm{t}^\pm} &= \pm\frac{1}{2w_0^2}\int_{-\infty}^{\infty}\mathrm{d}\xi\, \partial_\chi h^{(0)}_{\tau\zeta} + \frac{\theta}{2w_0^2}\int_{-\infty}^{\infty}\mathrm{d}\xi\, \partial_\chi h^{(1)}_{\xi\zeta} \\ &= \pm\frac{4\pi GP_0}{c^5}\,\mathrm{erf}\left(\sqrt{2}|\mu|\chi\right) + \lambda\frac{2\sqrt{2\pi}GP_0\theta}{c^5}|\mu|\mathrm{e}^{-2|\mu|^2\chi^2}.\end{aligned} \tag{11}$$

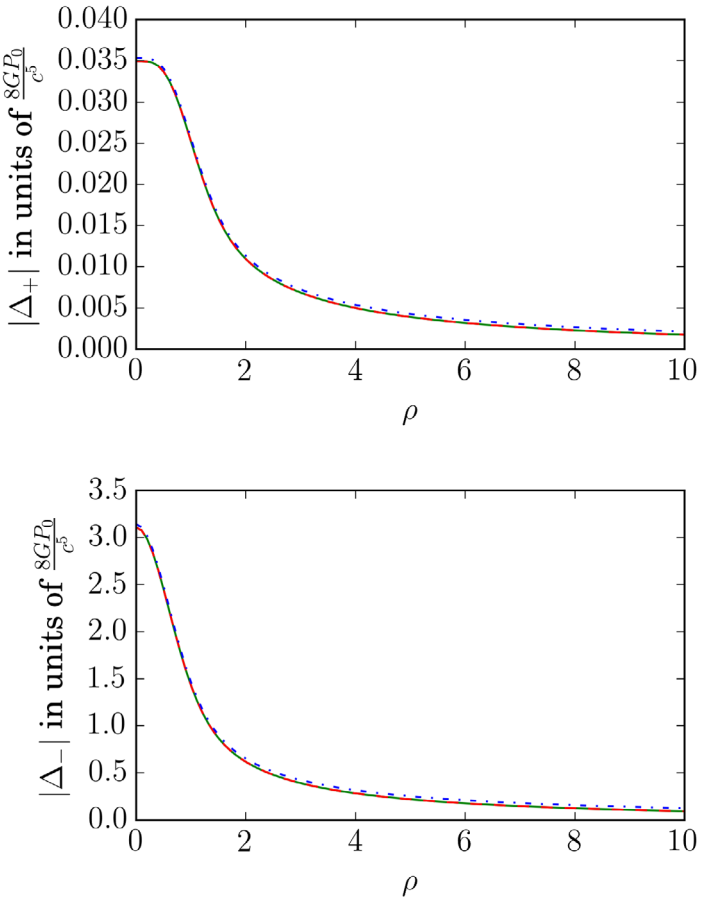

Figure 4. The absolute value of the polarization rotation angle Δ_+ (upper graph) for a parallel co-propagating light ray and Δ_- (lower graph) for a parallel counter-propagating light ray as a function of the transversal distance ρ from the beamline. The blue (dashed–dotted) line gives the rotation angle for the infinitely extended source beam and test ray. The green (unbroken) line gives the rotation angle for a source beam with emitter and absorber at $\zeta = -200$ and $\zeta = 200$, respectively, and infinitely extended test ray. The red (dashed) line gives the numerical values for the same extensions of the test beam and a finitely extended test light-ray with emitter (absorber) and absorber (emitter) at $\zeta = A = -600$ and $\zeta = B = 600$, respectively, for the co-propagating (counter-propagating) beam. For the parameters given in the introduction, the factor $8GP_0/c^5$ is of the order 10^{-37}. The plots show good agreement between our results for finitely and infinitely extended beams close to the beamline.

Let us denote the first term in equation (11) as $\Delta^{(0)}_{t^\pm}$ and the second term as $\Delta^{(1)}_{t^\pm}$. Then, we find that $\Delta^{(1)}_{t^\pm} = \frac{\lambda\theta}{4}\partial_\chi \Delta^{(0)}_{t^+}$. One might think that the symmetry of the beam geometry implies that $\Delta^{(0)}_{t^\pm}$ should vanish at $\zeta = 0$ as the term is independent of the helicity of the source beam. However, the symmetry is broken due to the direction of propagation of the source laser-beam. This can also be seen from the fact that only the $\tau\zeta$-component of the metric perturbation contributes to the effect, which would vanish for a massive medium at rest (see for example the Levi-Civita metric for an infinitely extended rod of matter [28]). The effect is similar to

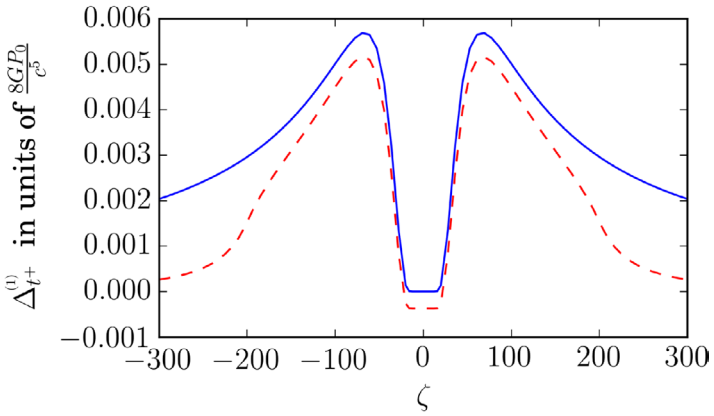

Figure 5. First order contribution (corresponding to the leading order effect of gravitational optical activity) to the rotation angle Δ_{t^+} for the polarization vector of an transversally propagating test ray with $\lambda = +1$: the blue, continuous line corresponds to the infinitely extended source beam, and the red, dashed line corresponds to the finitely extended source beam, emitted at $\alpha = -200$ and absorbed at $\beta = 200$. The test ray runs from $\xi = A = -600$ to $\xi = B = 600$ at $\chi = 10$. We find that the results for the infinitely extended source beam and test ray can be used to describe the effect in the case of the finitely extended source beam and test ray to some approximation for ζ-positions that are in between emitter and absorber, but far from them. It can be seen that the rotation decreases fast at the ends of the finitely extended source beam.

the deflection of a transversally propagating test ray, which is both deflected radially towards the laser beam as well as in ζ-direction [1]. To illustrate the ζ-dependence of $\Delta^{(1)}_{t^\pm}$, a numerical evaluation and a comparison to results for a finitely extended source beam (see the following subsection) are given in figure 5.

The first and the second term in equation (11) are fundamentally different in their dependence on the variable χ, which can be interpreted as the impact parameter of the scattering of the test light-ray with respect to the source beam. $\Delta^{(1)}_{t^\pm}$ is proportional to the same Gaussian function of χ that appears as a global factor in the energy-momentum tensor of the source beam for $\xi = 0$, which means that it vanishes if there is no overlap of the source beam and the test ray in the same way as in the case of Δ_+ and Δ_- above. Instead, the first term in equation (11) vanishes at $\chi = 0$ and saturates for large values of χ at a finite value, see figure 6 for plots showing numerical values for the first term in (11) and for the finitely extended source beam.

Up to numerical factors of order 1, the prefactors in equations (9)–(11) can be interpreted as the ratio of the power P_0 of the source laser-beam to the Planck power $E_p/t_p = E_p^2/\hbar$, where $E_p = \sqrt{\hbar c^5/G}$ is the Planck energy, which explains the smallness of the effect.

4.2. Finite versus infinite source beams and test rays and the long range behavior

For potential future experiments, finitely extended test-rays are relevant. It may even not be possible to realize extensions of the test ray much larger than that of the source beam or one may need to know details about the decay of the effect for large distances from the beamline. It should then be kept in mind that (7) holds for test rays that begin and end in flat spacetime. This is a condition which can be fulfilled only approximatively for a finitely extended test-ray. Furthermore, only under this condition has the rotation of the polarization a clear physical,

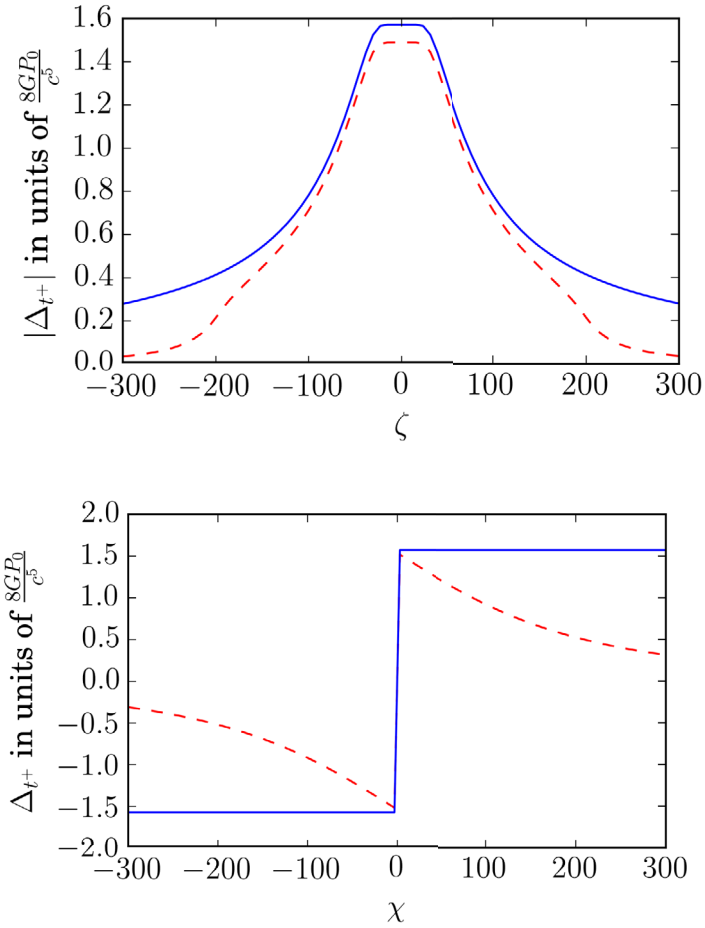

Figure 6. The rotation angle Δ_{t^+} (zeroth and first order) for the polarization vector of an transversally propagating test ray: the blue, plain line corresponds to the infinitely extended source beam, and the red, dashed line corresponds to the finitely extended source beam, emitted at $\alpha = -200$ and absorbed at $\beta = 200$. For the finitely extended source beam, the test ray is emitted at $\xi = A = -600$ and absorbed at $\xi = B = 600$. In the first plot, $|\Delta_{t^+}|$ is given as a function of the coordinate ζ along the beamline for $\chi = 10$. For the parameters given in the introduction, the factor $8GP_0/c^5$ is of the order 10^{-37}. We find that the results for the infinitely extended beam approximate those for the finitely extended beam for ζ-positions in between emitter and absorber that are far from emitter and absorber. It can be seen that $|\Delta_{t^+}|$ decays quickly outside of the range of the finitely extended source beam and test ray in contrast to $|\Delta_{t^+}|$ for the infinitely extended ones that always overlap. In both cases, the maximal effect is obtained close to $\zeta = 0$. In the second plot, the angle Δ_{t^+} is given as a function of χ at $\zeta = 0$. For large values of χ, it reaches a constant value for the infinitely extended source beam and test ray (undashed, blue) and decreases for the finitely extended source beam and test ray (dashed, red). A dependence on χ as $1/\chi^2$ is found for larger values of χ using a multipole expansion presented in appendix F.

coordinate-invariant meaning. To give a physical meaning to the rotation angle for a finitely extended test-ray, a physical reference system may be considered that extends from emitter to absorber. To this end, matter properties of the reference system like its density and stiffness have to be taken into account to obtain a reliable result. This is very similar to the considerations we made in [29] for the frequency shift of an optical resonator in a curved spacetime. We do not follow such an approach in this article.

Here we rather focus on the question under which conditions equation (7), when integrated over a finitely extended test ray, leads to results comparable to those of the infinitely extended test-ray. We will find that sufficiently close to the beamline the results from the finite integration can be very close to those of an infinite test-ray, which suggests that the latter, rigorous results with clear physical meaning, also remain valid for experiments using a finitely extended test-ray close to the source beam. The situation is quite different, however, in the far field, where results from the finite source beam and the infinitely extended one, both evaluated using (7), can differ siginificantly. This can be shown with a multipole expansion based on equation (6) or by numerically evaluating equation (6). The basic expressions for the numerics are given in appendix C and the multipole expansion is performed in appendix F. Here we briefly discuss both approaches and the main results.

The numerical values for the rotation angle for finitely extended test rays and source beams presented in figure 4 are obtained from equations (C.6) and (C.7). The derivative in equation (7) acting on the metric perturbation is shifted to the energy-momentum tensor by pulling it into the integral, using the symmetry of the function $|\vec{x}-\vec{x}'|$ to replace the derivative for an un-primed coordinate by a derivative for a primed coordinate and partial integration. The resulting expressions are evaluated using Python and the scypy.integrate.quad and scypy.integrate.romberg methods. The results for the finitely extended beam and those for the infinitely extended beam are very similar close to the beamline, see figure 4. The region in the ξ-χ-plane containing most of the energy of the source beam can be defined by a drop of its intensity by a factor e^{-2}, which implies a radius $w(\zeta)=\sqrt{1+(\theta\zeta)^2}$ of that region. In standard notions $w(\zeta)$ is called the width of the beam as a realistic beam is never infinitely extended in the transversal direction and is usually considered to extend only on length scales of the order of $w(\zeta)$. Equations (9) and (10) imply that there is only a significant rotation angle accumulated along an infinitely extended test ray if the latter overlaps with the region bounded by the source beam's width, as the integrands in equations (9) and (10) are proportional to the same Gaussian function that can be found as a global factor in the energy-momentum tensor of the source beam. In the following, we will call this situation an overlap of the test light ray and the source beam. That Δ_- and Δ_+ are only non-zero for an overlap of test ray and source beam is confirmed by equations (E.15) and (E.8), where a cut-off of the source beam's energy-momentum distribution is considered. For $\theta\zeta \gg 1$, we find that $w(\zeta)\approx\theta\zeta$. Therefore, a test ray at $\rho \gg 1$ overlaps with the source beam only in regions where $|\theta\zeta| > \rho$. For the infinitely extended source beam and test ray, there is always an overlap, but it does not need to be the case if at least one of the two beams has finite length.

Note that for large values of $\theta\zeta$, the energy-density of the source laser-beam is proportional to $(\theta\zeta)^{-2}$ (while transversally it decreases as a Gaussian with the distance to the beamline). The same is true for the integrands in equations (9) and (10). Therefore, $\Delta_\pm$ in equations (9) and (10) are approximately proportional to $1/(\theta\zeta)$ evaluated at the boundaries of the regions where test ray and source beam overlap. For the infinitely extended beams, this implies that the rotation angles in equations (9) and (10) are approximately proportional to $1/\rho$ for large ρ. The proportionality of Δ_- and Δ_+ to $1/\rho$ holds as well for finitely extended source beams if $\rho \ll -\theta\alpha$ or $\rho \ll \theta\beta$. For larger values of ρ, there is no overlap of test ray and source beam

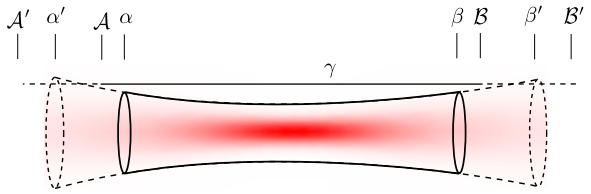

Figure 7. Illustration of the overlap of the test ray with the source laser-beam: A test ray may overlap with the source laser-beam only if the latter is long enough. In the illustration, the path of the test ray is labelled by γ and starts and ends at $\mathcal{A}$ and $\mathcal{B}$ respectively for the short source laser-beam (starting and ending at α and β respectively) or at $\mathcal{A}'$ and $\mathcal{B}'$ for the long source laser-beam (starting and ending at α' and β' respectively).

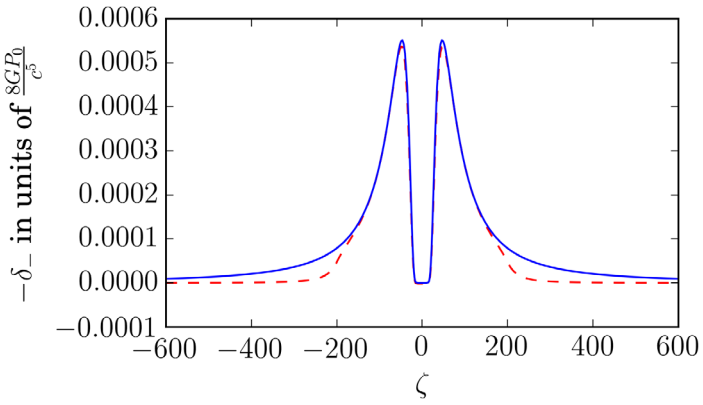

Figure 8. The function $-\delta_-$ (the integrand in equation (10)) for the polarization vector of the parallel counter-propagating light ray is plotted as a function of the coordinate along the beamline ζ for a distance from the beamline $\rho = 10$. The blue (unbroken) line gives the rotation angle for the infinitely extended source beam and test ray as in equation (10). The red (dashed) line gives the numerical values for a finitely extended source beam with emitter and absorber at $\alpha = -200$ and $\beta = 200$, respectively, based on (6). It can be seen that δ_- decays quickly outside of the range of the finitely extended beam in contrast to δ_- for the infinitely extended source beam, which continues to decay like $1/\zeta^2$ for large ζ just as the source beam's energy density. The region left of the steep descent around $\zeta \sim -70$ and the region right of the steep ascent around $\zeta \sim 70$ correspond to the overlap regions of source beam and test light-ray. In the case of an infinitely extended source beam, these regions are infinitely extended. In the case of a finitely extended source beam, the overlap regions end at the end of the source beam as can be seen with the steep ascent close to $\zeta = -200$ and the steep descent close to $\zeta = 200$ for the red (dashed) curve.

(this is illustrated in figure 7 and figure 8). Then, Δ_- and Δ_+ decay proportional to $\mathrm{e}^{-\Sigma\rho^2}/\rho^2$ and $\mathrm{e}^{-\Sigma\rho^2}$, respectively, where $\Sigma = 2/(\theta\alpha)^2$ for $\alpha \geqslant -\beta$ or $\Sigma = 2/(\theta\beta)^2$ for $\beta \geqslant -\alpha$, as shown in equation (E.11) and equation (E.17), respectively.

The behavior for large distances from the beamline and finitely extended test rays can be analysed with a multipole expansion, assuming that the source term in the form of the derivatives of the energy-stress tensor can be effectively cut-off at $w(\zeta)$. This is presented in appendix F. One finds that for $\Delta_\pm$ the lowest contributing moment is a quadrupole leading to a $1/\rho^3$ decay for finite $B = -A$. At the same time, the prefactor of these terms decay as

$1/B^2$ for $B \gg \rho$. Higher multipoles lead to an even faster decay, both with ρ and B. Hence, in the case of a finitely extended source beam and an infinitely extended test ray that does not overlap with the source beam, one expects to recover the fast decay of $\Delta_\pm$ with ρ obtained in equations (9) and (10). However, a resummation of the multipole expansion would be needed to find out its functional form. This is beyond the scope of the present investigation. Nevertheless, the analysis makes clear that $\Delta_\pm$ sensed by a finitely extended test ray in the far-field regime is not captured accurately by the results from the idealized infinitely extended test ray for the cases considered.

For the transversal test ray, the χ-dependence of $\Delta_{t\pm}$ for $\chi \gg 1$ changes drastically for the finitely extended source beam compared to the infinitely extended one. In particular, the result that the first term in equation (11) does not vanish for large distances from the beamline turns out to be an effect of the infinite extension of source beam and test ray. Alternatively, this can also be seen as follows: as $\Delta^{(0)}_{t\pm}$ is of zeroth order, it remains present when describing the laser beam in the paraxial approximation, in which the gravitational field of an infinitely extended source beam has the form $h_{00} = h_{33} = -h_{30} \propto \ln(\rho)$ (see [3, 30] and consider an infinite pulse length or see [2], consider an energy distribution localized to the beamline, and subtract the Minkowski metric from the resulting spacetime metric). From equation (7) and for a transversal infinitely extended test ray, we immediately obtain a rotation angle proportional to the first term in equation (11). On the other hand, the solution for the gravitational field for a finitely extended source beam can be found in [1]. In appendix G, using this solution and an infinitely extended test ray, we obtain the radial dependence of the rotation angle as $1/\chi$, and for a finitely extended test ray, we find that the rotation angle is proportional to $1/\chi^2$ for large χ. This is corroborated by the multipole expansion, where we find a monopole contribution responsible for the $1/\chi^2$ behavior to zeroth order in θ for $\chi \gg B$. As function of $B = -A$ it saturates for large B (i.e. $B \gg \chi$) and gives a β/χ behavior, see appendix F.

Since $\Delta^{(1)}_{t\pm} = \frac{\lambda\theta}{4}\partial_\chi \Delta^{(0)}_{t^+}$, we find that $\Delta^{(1)}_{t\pm}$ decays as $1/\chi^3$ for finitely extended source beams and test rays and as $1/\chi^2$ for finitely extended source beams and infinitely extended test rays. The corresponding multipole expansion is given in appendix F.

4.3. Rotation of polarization and gravitational spin–spin coupling

The rotation angles $\Delta_\pm$ as well as the first order contribution to $\Delta_{t\pm}$ are proportional to the helicity λ of the source laser-beam. As explained in the end of section 3, the rotation angle is equivalent to a phase for circularly polarized test light rays, which is given by $-\lambda_{\text{test}}\Delta$. This phase contains the product of the helicities of the source laser-beam and the test ray, $\lambda\lambda_{\text{test}}$. Therefore, the phase depends on the relative helicity of the two beams. This is gravitational spin–spin coupling.

We can consider the source beam as its own test beam, $\lambda_{\text{test}} = \lambda$, such that $\lambda_{\text{test}}\Delta_+ = C_+$ where $C_+ > 0$ is a function that increases monotonously with the end of the source beam at $\zeta = \beta$ (see (9)). Since C_+ enters as a phase $\text{Exp}(\text{i}C_+)$, it can be combined with the global plane wave factor at the end of the beam $\zeta = \beta$ as $\text{Exp}(\text{i}\Phi)$ where $\Phi = 2(\beta - \tau)/\theta + C_+$. This leads to the locally modified wave number $\tilde{k} = \partial_\beta\Phi = (2 + \theta\,\partial_\beta C_+)/\theta$ at $\zeta = \beta$. Effectively, this leads to the interpretation of a locally modified dispersion relation and an effectively reduced speed of light. This self-interaction effect is proportional to the intensity of the electromagnetic field. It is reminiscent of the apparent modification of the speed of light found in [31] based on the eikonal approximation of the solution of the relativistic wave equation of a light-beam in its own gravitational field.

5. Faraday effect and optical activity

The electromagnetic Faraday effect is a non-reciprocal phenomenon. Non-reciprocity means that the effect does not cancel when the test ray propagates back and forth along the same path. We investigate this feature for its gravitational analogue.

The rotation angle given in equation (7) is defined with respect to the propagation direction. Therefore, the absolute rotation accumulated on the way back and forth through spacetime seen by an external reference system at the starting point of the test ray's trajectory at spatial infinity is given by the difference between the rotation angle acquired on the outbound trip and the one acquired on the way back. For a tangent vector t_0^μ with $t_0^0 = 1$ and $t_0^a = \mathrm{d}\, s^a$ with $d = +1$ for outbound and $d = -1$ for back propagation, we obtain from equation (7) the rotation angle

$$\Delta_{s,d} = \frac{1}{2w_0^2}\int_{-\infty}^{\infty} \mathrm{d}\tau\; s^a \epsilon_{abc}\partial_b (h_{cf} s^f + \mathrm{d} h_{c\tau}), \tag{12}$$

and therefore, the Faraday rotation for one roundtrip becomes

$$\Delta_s^{\mathrm{F}} = \Delta_{s,+} - \Delta_{s,-} = \frac{1}{w_0^2}\int_{-\infty}^{\infty} \mathrm{d}\tau\; s^a \epsilon_{abc}\partial_b h_{c\tau}. \tag{13}$$

We find that the gravitational Faraday effect is given by the spacetime-mixing component of the metric perturbation $h_{c\tau}$. In contrast, the first term in (12) containing a purely spatial component of the metric perturbation does not depend on the propagation direction and cancels on the way back and forth. This is the gravitational optical activity for a single trip

$$\Delta_s^{\mathrm{Op}} = \frac{\Delta_{s,+} + \Delta_{s,-}}{2} = \frac{1}{2w_0^2}\int_{-\infty}^{\infty} \mathrm{d}\tau\; s^a s^d \epsilon_{abc}\partial_b h_{cd}. \tag{14}$$

For the rotation due to the gravitational Faraday effect after one roundtrip for the parallel test ray, we obtain from equation (8) to leading order

$$\begin{aligned}\Delta_{+-}^{\mathrm{F}} &= \Delta_+ - \Delta_- \\ &= -\frac{\theta}{w_0^2}\int_{-\infty}^{\infty} \mathrm{d}\zeta \left(\partial_\chi h_{\tau\xi}^{(1)} - \partial_\xi h_{\tau\chi}^{(1)}\right).\end{aligned} \tag{15}$$

Adding the rotations due to the transversal back and forth propagation leads to (the explicit expression is identical to twice the positive contribution of the first term in equation (11)),

$$\Delta_{\mathrm{t}^+\mathrm{t}^-}^{\mathrm{F}} = \Delta_{\mathrm{t}^+} - \Delta_{\mathrm{t}^-} = \frac{1}{w_0^2}\int_{-\infty}^{\infty} \mathrm{d}\xi\; \partial_\chi h_{\tau\zeta}^{(0)}, \tag{16}$$

which means that the effect is of zeroth order. The contribution of gravitational optical activity is given as (to leading order and for one direction of propagation)

$$\begin{aligned}\Delta_{+-}^{\mathrm{Op}} &= \frac{\Delta_+ + \Delta_-}{2} \\ &= -\frac{\theta}{2w_0^2}\int_{-\infty}^{\infty} \mathrm{d}\zeta \left(\partial_\chi h_{\zeta\xi}^{(1)} - \partial_\xi h_{\zeta\chi}^{(1)}\right)\end{aligned} \tag{17}$$

for the parallel test rays, and

$$\Delta_{\mathrm{t}^+\mathrm{t}^-}^{\mathrm{Op}} = \frac{\Delta_{\mathrm{t}^+} + \Delta_{\mathrm{t}^-}}{2} = \frac{\theta}{2w_0^2}\int_{-\infty}^{\infty} \mathrm{d}\xi\; \partial_\chi h_{\xi\zeta}^{(1)} \tag{18}$$

for the transversal test rays.

From the vanishing of Δ_+ in first order in the metric perturbation, we deduce that the first order contributions of optical activity and the Faraday effect to the polarization rotation accumulated along a parallel co-propagating test ray have the same absolute value and cancel each other. In contrast, the two contributions add for the counter-propagating test ray. This situation can be compared to the result of Tolman *et al* [1], which states that a test ray is not deflected in the gravitational field of a source light-beam if it is parallel co-propagating, while it is deflected if it is parallel counter-propagating. It is the motion of the source of gravity that breaks the symmetry; its motion with the speed of light leads to the extreme case of equal absolute values of the two effects.

5.1. Spacetime-medium analogy

The above identification of the two distinct rotation effects and the different types of components of the metric perturbation can be compared with the formal analogy of electrodynamics in linear dielectric media and electrodynamics in a weakly curved spacetime employed in [8]. In particular, Maxwell's equations in a curved spacetime can be rewritten such that they have their usual form in dielectric media [8]

$$-\partial_t D_a + \epsilon_{abc}\partial_b H_c = i_a, \tag{19}$$

$$\partial_t B_a + \epsilon_{abc}\partial_b E_c = 0, \tag{20}$$

$$\partial_a D_a = \rho, \quad \partial_a B_a = 0 \tag{21}$$

by identifying the components of the field strength tensor as

$$E_a = cF_{a0} \tag{22}$$

$$B_a = \frac{1}{2}\epsilon_{abc}F_{bc} \tag{23}$$

$$D_a = \varepsilon_0 c\sqrt{-g}g^{0\mu}g^{a\nu}F_{\mu\nu} \tag{24}$$

$$H_a = \frac{1}{2\mu_0}\epsilon_{abc}\sqrt{-g}g^{b\mu}g^{c\nu}F_{\mu\nu} \tag{25}$$

and $i_a = \sqrt{-g}j^a$ and $\rho = \sqrt{-g}j^0/c$, where j^μ is the current density, $\sqrt{-g}$ is short for $\sqrt{-\det(g)}$ and g is the spacetime metric. This leads to an effective constitutive law

$$D_a = \varepsilon_{ab}E_b + \epsilon_{abc}\Xi_b H_c, \tag{26}$$

$$B_a = \mu_{ab}H_b + \epsilon_{abc}\Upsilon_b E_c, \tag{27}$$

where[8]

$$\varepsilon_{\mathrm{r},ab} = \mu_{\mathrm{r},ab} = -\frac{\sqrt{-g}}{g_{\tau\tau}}g^{ab}, \tag{28}$$

$$\Xi_a = -\Upsilon_a = \frac{g_{\tau a}}{cg_{\tau\tau}}, \tag{29}$$

[8] Note that what we define as ϵ is the effective permittivity tensor in contrast to [8], where the identity is subtracted.

where $\varepsilon_{\mathrm{r},ab} = \varepsilon_{ab}/\varepsilon_0$ and $\mu_{\mathrm{r},ab} = \mu_{ab}/\mu_0$ are the relative permittivity tensor and relative permeability tensor, respectively. In the above identification, purely spatial components of the metric perturbation lead to non-trivial effective relative permittivity and permeability tensors while space-time mixing components of the metric perturbation lead to effective non-vanishing magneto-electrical mixing terms. Note the equivalence of the effective relative permittivity and permeability tensors, denoted as impedance matching [32], which is usually not encountered in materials.

In linearized gravity using $\eta = w_0^2\mathrm{diag}(-1,1,1,1)$ and the set of coordinates τ, ξ, χ and ζ, we find

$$\varepsilon_{\mathrm{r},ab} = \mu_{\mathrm{r},ab} = \delta^{ab}\left(1 + \frac{h_{\tau\tau} + \delta^{cd}h_{cd}}{2w_0^2}\right) - \frac{h_{ab}}{w_0^2}, \tag{30}$$

$$\Xi_a = -\Upsilon_a = -\frac{h_{\tau a}}{cw_0^2}. \tag{31}$$

We obtain for the gravitational Faraday rotation angle from equation (13)

$$\begin{aligned}\Delta_s^{\mathrm{F}} &= -c\int_{-\infty}^{\infty} \mathrm{d}\tau\; s^m \epsilon_{mab}\partial_a \Xi_b \\ &= -c\int_{-\infty}^{\infty} \mathrm{d}\tau\; s^m (\nabla\times\Xi)_m.\end{aligned} \tag{32}$$

We see that the gravitational Faraday rotation is induced by the curl of the magneto-electrical mixing vector Ξ; it is a magneto-optical effect like its analogue in dielectric media. For the gravitational optical activity, we obtain from equation (14)

$$\begin{aligned}\Delta_s^{\mathrm{Op}} &= -\frac{1}{2}\int_{-\infty}^{\infty} \mathrm{d}\tau\; s^m s^d \epsilon_{mbc}\partial_b \varepsilon_{\mathrm{r},cd} \\ &= -\frac{1}{2}\int_{-\infty}^{\infty} \mathrm{d}\tau\; s^a s^b \left(\nabla\times\varepsilon_{\mathrm{r}}\right)_{ab}.\end{aligned} \tag{33}$$

We find that the gravitational optical activity is induced by a non-vanishing curl of the lines (or columns) of the permittivity tensor (and, equivalently, the permeability tensor). In analogy to the optical activity in dielectric media, the gravitational optical activity does not mix electric and magnetic fields.

For the gravitational field of the laser beam in appendix A, we obtain evaluated up to first order in θ

$$\varepsilon_{\mathrm{r},ab} = \mu_{\mathrm{r},ab} = \begin{pmatrix} 1 + \frac{h^{(0)}_{\zeta\zeta}}{w_0^2} & 0 & -\frac{\theta h^{(1)}_{\xi\zeta}}{w_0^2} \\ 0 & 1 + \frac{h^{(0)}_{\zeta\zeta}}{w_0^2} & -\frac{\theta h^{(1)}_{\chi\zeta}}{w_0^2} \\ -\frac{\theta h^{(1)}_{\xi\zeta}}{w_0^2} & -\frac{\theta h^{(1)}_{\chi\zeta}}{w_0^2} & 1 \end{pmatrix} \tag{34}$$

$$\Xi_j = -\Upsilon_j = -\frac{\theta h^{(1)}_{\tau j}}{cw_0^2}, \text{ where } j \in \{\xi, \chi\} \tag{35}$$

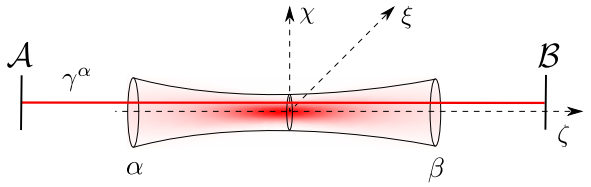

Figure 9. Schematic illustration of the parallel cavity in the gravitational field of the laser beam: the source laser-beam starts at α and ends at β. The test ray propagates on the worldline γ between the mirrors $\mathcal{A}$ and $\mathcal{B}$ of the cavity. The Faraday effect adds up after each roundtrip, while the rotation associated with gravitational optical activity vanishes.

$$\Xi_\zeta = -\Upsilon_\zeta = -\frac{h^{(0)}_{\tau\zeta}}{cw_0^2}, \tag{36}$$

and we recover the results in equations (15)–(18).

6. Test rays in cavities

In this section, we will consider the situation of the test light-ray propagating in a cavity. In a one-dimensional cavity light propagates back and forth and the effect associated with gravitational optical activity cancels while the gravitational Faraday effect adds up. In a ring cavity or an optical fiber coiled around the beamline, the full polarization rotation is accumulated and the gravitational Faraday effect represents the leading order effect. For the case of a transversally oriented ring cavity, a situation can be created in which the Faraday effect vanishes and only the gravitational optical activity accumulates.

6.1. Parallel linear cavity

We consider a cavity consisting of two mirrors between which the light propagates back and forth, with the axis of the cavity oriented parallel to the beamline and at a distance ρ from the beamline. The setup is illustrated in figure 9.

Up to third order in θ, the light travels undeflected from $\zeta = A$ to $\zeta = B$ and picks up a small deflection of zeroth order in θ when travelling from $\zeta = B$ to $\zeta = A$. The deflection vanishes when the light ray propagates at the center of the source beam, at $\rho = 0$. In this case only the angle due to the Faraday effect accumulates. For one back and forth propagation, it is given by equation (15). Letting the light propagate during the time $\tau = LF/(\pi c)$, where F is the finesse of the cavity and L is the length of the cavity, the total angle of rotation is given by $\Delta_{\text{cav},+-} = \Delta^{\text{F}}_{+-}F/(2\pi)$. For a cavity of finesse $F = 10^6$ [33] and the parameters given in the introduction, i.e. beam waist $w_0 = 10^{-6}$ m, beam divergence $\theta = 0.3$ rad, polarization $\lambda = 1$, and power of the source laser-beam $P_0 = 10^{15}$ W, the rotation angle accumulated by the test-ray in the cavity is of the order of magnitude $\Delta_{\text{cav},+-} \sim \pm 10^{-32}$ rad. For a cavity at distance $\rho > 0$ from the center of the laser beam, the effect is smaller, and one has to take into consideration the deflection when the test ray is counter-propagating to the source laser-beam.

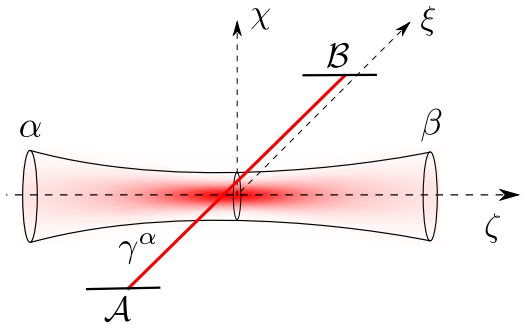

Figure 10. Schematic illustration of the transversal cavity in the gravitational field of the laser beam: the test ray propagates along the worldline γ, marked as a red line, and is reflected at the mirrors $\mathcal{A}$ and $\mathcal{B}$. The source laser-beam is emitted at $\zeta = \alpha$ and absorbed at $\zeta = \beta$. The Faraday effect adds up after each roundtrip, while the rotation associated with gravitational optical activity vanishes.

6.2. Transversal linear cavity

Rotating the parallel cavity by ninety degrees, we obtain a transversal cavity, as illustrated in figure 10. Analogously to the parallel cavity, one finds that the total angle of rotation is given by $\Delta_{\text{cav,t+t-}} = \Delta^{\text{F}}_{\text{t+t-}} F/(2\pi)$. For a finesse of $F \sim 10^6$ and the parameters given in the introduction, it is of the order $\pm 10^{-32}$ rad.

6.3. Ring cavity

In order to measure the polarization rotation including the contribution due to optical activity for the transversal light ray, we consider a ring cavity: the light propagates from $\mathcal{A}$ at $(\xi, \chi, \zeta) = (-\infty, \chi_1, 0)$, to $\mathcal{B}$ at $(\xi, \chi, \zeta) = (\infty, \chi_1, 0)$, to $\mathcal{C}$ at $(\xi, \chi, \zeta) = (\infty, \chi_2, 0)$, where χ_1 and χ_2 have opposite sign, to $\mathcal{D}$ at $(\xi, \chi, \zeta) = (-\infty, \chi_2, 0)$ and back to $\mathcal{A}$. The $\pm\infty$ can be replaced by distances from the beamline much larger than β. The polarization rotation accumulated when propagating from $\mathcal{A}$ to $\mathcal{B}$ and from $\mathcal{C}$ to $\mathcal{D}$ add up. The setup is illustrated in figure 11.

The rotation of polarization after one roundtrip is given by twice the expression in equation (11) for $\chi_1 \sim 1$ and $\chi_2 \sim -1$. For $\chi_1 \gg \beta$, $\chi_2 \gg -\beta$ and $\alpha = -\beta$, we have shown that the effect decays as β/χ^2 in appendix F. As the first term in equation (11) corresponding to the gravitational Faraday effect is of zeroth order in θ, it does not depend on the beam waist for the fixed wavelength given by $\pi\theta w_0$. This means that the beam has to be long, but it does not need to be focused. Again for a finesse of $F = 10^6$ and the parameters given in the introduction, the rotation is of the order of magnitude $\Delta_{\text{t+}} F/(2\pi) \sim 10^{-32}$ rad.

For $\chi_1 = 0$ and $\chi_2 = -\infty$ or at least $-\chi_2$ very large, we find that the polarization rotation due to the Faraday effect vanishes (see also equation (E.22)) and the rotation due to gravitational optical activity remains (see also equation (E.23)). Then, the accumulated effect is by one order smaller than that due to the Faraday effect at $\chi_1 = \chi_2 > 1$.

A ring cavity can also be used to amplify the rotation angle of the polarization the parallel co-propagating test ray acquires: since it is not deflected, one can let the light ray pass through the gravitational field N times just in the direction of propagation of the source beam, such that the effect is amplified by a factor N.

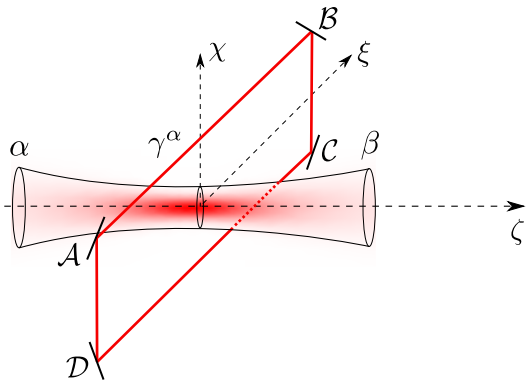

Figure 11. Schematic illustration of the ring cavity setup: the test ray propagates along the path γ and is reflected at the mirrors $\mathcal{A}$, $\mathcal{B}$, $\mathcal{C}$ and $\mathcal{D}$. The source laser-beam is emitted at $\zeta = \alpha$ and absorbed at $\zeta = \beta$. A similar situation can be created with a test ray in a wave guide that is wound many times around the source beam.

6.4. Measurement precision of the rotation angle

The rotation angle Δ is experimentally inferred by measuring the additional phase difference that the right- and left-circularly polarized components of the test ray acquire when propagating in the gravitational field as explained in the end of section 3. The measurement precision of the phase $\Phi = -\lambda_{\text{test}}\Delta$ is restricted by the shot noise. Using classical light, the minimal uncertainty in a phase estimation cannot exceed the shot noise limit, which is of the order of magnitude $\delta\Phi \sim \frac{1}{\sqrt{nM}}$, where n is the number of photons of the light inside the cavity and M the number of measurements [34]. For a cavity resonator driven by a laser with frequency $\omega/(2\pi)$ and power P_{dr}, we find a number of photons $n = P_{\text{dr}}T_{\text{av}}/(\hbar\omega)$, where T_{av} is the average time a photon spends in the resonator. Therefore, the number of measurements that can be performed with n photons in an experimental time T_{tot} is given as $M = T_{\text{tot}}/T_{\text{av}}$, giving $nM = P_{\text{dr}}T_{\text{tot}}/(\hbar\omega)$, which is the total number of photons passing the cavity in time T_{tot}.

The measurement precision becomes thus better by increasing the power of the driving laser and lowering its frequency. For cw-laser beams with power $P_{\text{dr}} = 100$ kW [35][9], for a wavelength of approximately 500 nm and a total experimental time of about two weeks, i.e. $T_{\text{tot}} \sim 10^6$ s, the minimal standard deviation is given by $\delta\Phi \sim 10^{-15}$ rad. Its order of magnitude does not change when using a squeezed (single mode coherent) state with the currently maximal squeezing of 15 dB [37][10] and analyzing the uncertainty with the corresponding quantum Cramér-Rao bound [38].

[9] Of course the power of the driving laser cannot be unlimited as the cavity mirrors have to withstand the heating due to scattered light. The finesse $F \sim 10^6$ leads to a circulating power in the cavity of the order of 10^{10} W, which leads to a necessary size of the beam at the mirrors of the order of 1 m [36]. Assuming the transversal setup described in section 6, the waist of the test ray has to be smaller than the waist of the source beam and the divergence angle of the test ray must be smaller than one radian to ensure a complete overlap of the focal regions of the source beam and the test ray. We assumed a waist of the source beam of the order of 10^{-6} m, which implies a maximum waist of the test ray of the same order. Furthermore, the divergence angle of the test ray below one radian implies that the distance between the mirrors of the test ray has to be of the order of several meters. The situation for the longitudinal cavity turns out to be even more challenging. However, the given parameters serve as an upper limit of what would be possible in the near future.

[10] Note that this degree of squeezing has only been reached for much a smaller beam power of the order of mW, which would actually lead to a decrease in the sensitivity.

The Cramér-Rao bound is a tight bound on the uncertainty of an unbiased phase-estimation that can in principle be achieved in a highly idealized situation, where all other noise sources such as thermal noise, electronic noise, seismic noise etc are neglected. The sensitivity can be increased by using more than one mode, but without entangling the modes or creating other non-classical states no gain in sensitivity at fixed total energy is possible [39].

For a more practical benchmark of current state-of-the-art measurement precision, consider the LIGO observatory. It obtains a sensitivity for length changes of their arms of the order of 10^{-20} m (strains of the order of $10^{-23}\,(\mathrm{Hz})^{-1/2}$ on an arm length of the order of 10^{3} m [40]), which corresponds to a phase sensitivity of the order of 10^{-11} rad at about 1000 nm wavelength. Another obstacle is that the source-laser power of 10^{15} W that we considered here can so far only be reached in very short pulses, which means that an extension of our analysis to pulsed source beams will be required when one day substantially larger powers and more sensitive measurements might become available. We conclude that the angles due to the gravitational Faraday effect of the order of magnitude $\Delta \sim 10^{-32}$ rad cannot be measured with current and near-future technology.

7. Summary, conclusion and outlook

We analyzed the rotation of polarization for a test ray propagating in the gravitational field of a laser beam. We distinguished the non-reciprocal contribution to the rotation due to the gravitational Faraday effect from the reciprocal contribution associated with the gravitational optical activity. As the rotation angle is equivalent to a phase for circularly polarized test rays, the precision of the measurement of the effect investigated in this article is limited by the shot-noise limit when using classical light. With this analysis we found that the rotation of polarization of a test ray induced by the gravitational field of a circularly polarized source laser-beam is too small to be measured with state-of-the-art technology. The effects are of fundamental interest, however.

For an infinitely extended (or at least very long) test ray propagating parallel to the source beam, we found that the local rotation picked up by the polarization vector of the test ray is proportional to the energy density of the source beam. In that case, we concluded that effects are only present for an overlap of the test ray and the source beam's region of highest intensity bounded by its width. Using the approximation of an infinitely extended source beam, such an overlap is always present for parallel propagating test rays and we find a decay of the integrated rotation angle with the inverse of the distance to the beamline of the source beam. In the realistic situation of a finitely extended source beam, this dependence on the distance remains approximately valid as long as there is a significant overlap. However, for the finitely extended source beam, there is no overlap for distances from the beamline larger than the extension of the beamline multiplied by the divergence angle of the source beam. Above that limit, we find that the polarization rotation picked up by a parallel propagating infinitely extended test ray decreases as a Gaussian with the distance to the beamline of the source beam. For a finitely extended test ray far from the beamline of the source beam, we find that the effects decay with the inverse of the third power of the distance using a multipole expansion. However, a finitely extended test ray begins and ends in regions with non-vanishing gravitational effect of the source beam. Hence, the interpretation of the rotation angle is not straight forward. To overcome this problem, a physical reference system could be considered that extends or is moved from the beginning to the end of the test ray.

For transversally propagating test rays, the situation is different: the leading order effect decreases with the inverse of the distance from an finitely extended source beam for an infinitely extended test ray and with the inverse square for a finitely extended test ray. Therefore, of the effects investigated in this article, the rotation of polarization of a transversal test ray should be the easiest to detect, while we reiterate that a detection will not be possible in the near future. It is interesting to note that the effect remains there also in the geometric optical limit and is independent of the source beam's helicity.

Only the gravitational Faraday effect contributes to the leading order effect for the transversal test ray. The gravitational optical activity induces the next to leading order term, and it decays one order more strongly with χ than the gravitational Faraday effect.

It has been shown that for light passing through or being emitted from a rotating spherical body [6, 7] or a rotating spherical shell [12], one obtains a rotation of the polarization proportional to the inverse of the square of the distance to the rotating object. On the other hand, when the light ray is only passing by these objects or any stationary object, there is no rotation of polarization [41, 42, 42]. However, if these objects are in motion, it has been shown that the polarization is rotated (for a moving point mass [11], for gravitational lenses [10, 42], for a moving Schwarzschild object [9], for moving stars [8]). As the laser beam, although its spacetime metric is stationary, consists of an energy-distribution in motion, our results agree with the literature in the sense that the rotation of polarization is non-vanishing.

As another interesting fundamental insight, we found that to first order in the divergence angle θ, the polarization vector of a parallel counter-propagating test ray rotates, while this is not the case for a co-propagating test ray. We argue that this asymmetry is due to the propagation of the source laser-beam. This is similar to the deflection of a parallel test ray by the gravitational field of a laser beam which is non-zero for a counter-propagating ray and vanishes for a co-propagating ray [1].

The gravitational field of the laser beam depends on its polarization. This is in agreement with the gravitational field of a polarized infinitely thin laser beam or pulse derived in [3] and the gravitational field of a polarized electromagnetic plane wave presented in [43]. However, the gravitational field in the models [3, 43] does not depend on the direction of linear polarization and neither on the helicity of light in the case of circular polarization. This is in contrast to gravitational photon-photon scattering in perturbative quantum gravity discussed in [44]. In [5], we showed that the gravitational field of a laser beam considered as a proper perturbative solution of Maxwell's equations beyond the short wavelength approximation does depend on the helicity of the laser beam. In the present article, we showed that, accordingly, the polarizations of two light beams couple gravitationally; two circularly polarized light beams inflict on each other a phase shift depending on the relation between their helicity. This is gravitational spin–spin coupling of light (see [45] for a general review on gravitational spin–spin coupling).

Together with frame-dragging and the deflection of a parallel co-propagating test ray discussed in [5], the gravitational Faraday effect and gravitational optical activity are only visible when the source is treated beyond geometric ray optics. It can be expected that orbital angular momentum of light would contribute to the effects mentioned above. See [4, 46] for an investigation of the gravitational field of light beams with orbital angular momentum.

The situation considered in [46] and [47] of a spinning test particle can also be considered for the solution derived in [5]. This could be an interesting extension of the present article.

Acknowledgments

We thank Marius Oancea for helpful remarks and discussions and Julien Fraïsse for proof-reading the manuscript. DR would like to thank the Humboldt Foundation for supporting his work with their Feodor Lynen Research Fellowship.

Appendix A. Metric perturbation (from [5])

In this appendix, we give the explicit expressions for the metric perturbation as derived in [5]. The metric perturbation is obtained from the electromagnetic field of a circularly polarized laser beam given in [5], which is determined by the vector potential $A_\alpha(\tau,\xi,\chi,\zeta) = \tilde{\mathcal{A}} v_\alpha(\xi,\chi,\theta\zeta)\mathrm{e}^{\mathrm{i}\frac{2}{\theta}(\zeta-\tau)}$, where $\tilde{\mathcal{A}}$ is the amplitude, $v_\alpha = \sum_{n=0}^{\infty}\theta^n v_\alpha^{(n)}$ is the envelop function, whose spatial components, $a \in \{\xi,\chi,\zeta\}$, are given up to third order in θ by

$$v_a^{\lambda(0)} = \epsilon_a^{(0)} v_0, \tag{A.1}$$

$$v_a^{\lambda(1)} = -\epsilon_a^{(1)} \frac{\mathrm{i}\mu}{2\sqrt{2}} \left(\xi - \mathrm{i}\lambda\chi\right) v_0, \tag{A.2}$$

$$v_a^{\lambda(2)} = \frac{\mu}{2}\left(1 - \frac{1}{2}\mu^2\rho^4\right) v_a^{\lambda(0)}, \tag{A.3}$$

$$v_a^{\lambda(3)} = \frac{\mu}{4}\left(4 + \mu\rho^2 - \mu^2\rho^4\right) v_a^{\lambda(1)}, \tag{A.4}$$

where $\mu = 1/(1+\mathrm{i}\theta\zeta)$, the function v_0 is given by

$$v_0(\xi,\chi,\theta\zeta) = \mu \mathrm{e}^{-\mu\rho^2}, \tag{A.5}$$

and $\epsilon_a^{(0)} = w_0(1,-\lambda i,0)/\sqrt{2}$, $\epsilon_a^{(1)} = w_0(0,0,1)$ and $\lambda = \pm 1$ refers to the helicity. Since we work in the Lorenz gauge, the τ-component of the vector potential is given as

$$A_\tau = \frac{\mathrm{i}\theta}{2}\partial_\tau A_\tau = \frac{\mathrm{i}\theta}{2}\left(\partial_\xi A_\xi + \partial_\sigma A_\sigma + \theta\partial_{\theta\zeta} A_\zeta\right). \tag{A.6}$$

The leading order is thus the usual expression for the electromagnetic field of the Gaussian beam in the paraxial approximation. The higher orders are corrections to the paraxial approximation. The corresponding components of the energy-momentum tensor are given as $T_{\tau\tau} = \mathcal{E}$, $T_{\tau j} = -S_j/c$ and $T_{jk} = \sigma_{jk}$ for $j,k \in \{\xi,\chi,\zeta\}$. For the vector potential of a circularly polarized laser beam given by equation (A.1), the energy density $\mathcal{E}$, the Poynting vector $\vec{S}$ and the stress tensor components σ_{jk} up to third order in θ are given as

$$\mathcal{E}^\lambda = \mathcal{E}^{(0)}\left[1 + \frac{|\mu|^2\theta^2}{2}\left(1 + |\mu|^2(2 - (4|\mu|^2 - 3)\rho^2)\rho^2\right)\right], \tag{A.7}$$

$$S^{\lambda}_{\xi}/c = \mathcal{E}^{(0)}\theta|\mu|^2\Bigg[(\theta\zeta\xi+\lambda\chi) - \frac{\theta^2}{4}\Bigg(\lambda\chi - 2|\mu|^2\Bigg((2-\rho^2)\theta\zeta\xi + 2(1-\rho^2)\lambda\chi + (\theta\zeta\xi+\lambda\chi)(4+3\rho^2-4|\mu|^2\rho^2)|\mu|^2\rho^2\Bigg)\Bigg)\Bigg], \tag{A.8}$$

$$S^{\lambda}_{\chi}/c = -\lambda\mathcal{E}^{(0)}\theta|\mu|^2\Bigg[(\xi-\theta\zeta\lambda\chi) - \frac{\theta^2}{4}\Bigg(\xi - 2|\mu|^2\Bigg(2(1-\rho^2)\xi - (2-\rho^2)\theta\zeta\lambda\chi + (\xi-\theta\zeta\lambda\chi)(4+3\rho^2-4|\mu|^2\rho^2)|\mu|^2\rho^2\Bigg)\Bigg)\Bigg], \tag{A.9}$$

$$S^{\lambda}_{\zeta}/c = \mathcal{E}^{\lambda} - \frac{1}{2}\mathcal{E}^{(0)}(\theta\rho|\mu|)^2, \tag{A.10}$$

$$\sigma^{\lambda}_{\xi\xi} = \mathcal{E}^{(0)}\theta^2|\mu|^4(\theta\zeta\xi+\lambda\chi)^2, \tag{A.11}$$

$$\sigma^{\lambda}_{\chi\chi} = \mathcal{E}^{(0)}\theta^2|\mu|^4(\xi-\theta\zeta\lambda\chi)^2, \tag{A.12}$$

$$\sigma^{\lambda}_{\xi\chi} = \mathcal{E}^{(0)}\lambda\theta^2|\mu|^4(\theta\zeta\xi+\lambda\chi)(\theta\zeta\lambda\chi-\xi), \tag{A.13}$$

$$\sigma^{\lambda}_{\xi\zeta} = S^{\lambda}_{\xi}/c - \mathcal{E}^{(0)}\frac{\theta^3}{2}(\theta\zeta\xi+\lambda\chi)|\mu|^4\rho^2, \tag{A.14}$$

$$\sigma^{\lambda}_{\chi\zeta} = S^{\lambda}_{\chi}/c + \lambda\mathcal{E}^{(0)}\frac{\theta^3}{2}(\xi-\theta\zeta\lambda\chi)|\mu|^4\rho^2, \tag{A.15}$$

$$\sigma^{\lambda}_{\zeta\zeta} = \mathcal{E}^{\lambda} - \mathcal{E}^{(0)}(\theta\rho|\mu|)^2, \tag{A.16}$$

where $|\mu|^2 = 1/(1+(\theta\zeta)^2)$ and $\mathcal{E}^{(0)} = \varepsilon_0 w_0^2 E_0^2|v_0|^2 = 2P_0|\mu|^2\mathrm{Exp}(-2|\mu|^2\rho^2)/(\pi c)$.

A.1. Field equations

The linearized Einstein equations take the form

$$\Delta_{2d}h^{\lambda(0)}_{\alpha\beta} = -\kappa w_0^2\, t^{\lambda(0)}_{\alpha\beta}, \tag{A.17}$$

$$\Delta_{2d}h^{\lambda(1)}_{\alpha\beta} = -\kappa w_0^2\, t^{\lambda(1)}_{\alpha\beta}, \tag{A.18}$$

$$\Delta_{2d}h^{\lambda(n)}_{\alpha\beta} = -\kappa w_0^2\, t^{\lambda(n)}_{\alpha\beta} - \partial^2_{\theta\zeta}h^{\lambda(n-2)}_{\alpha\beta} \text{ for } n>1, \tag{A.19}$$

where $t^{(n)}_{\alpha\beta}$ are the coefficients of the power series expansion of the energy-momentum tensor in orders of θ, i.e. $T_{\alpha\beta} = \sum_n \theta^n t^{(n)}_{\alpha\beta}$.

A.2. Zeroth order

The metric perturbation in the leading (zeroth) order of the expansion in the beam divergence is given by [5]

$$h_{\tau\tau} = h_{\zeta\zeta} = -h_{\tau\zeta} = I^{(0)}, \tag{A.20}$$

where the function $I^{(0)}$ is given by

$$I^{(0)} = \frac{8GP_0w_0^2}{c^5}\left(\frac{1}{2}\mathrm{Ei}\left(-2|\mu|^2\rho^2\right) - \log(\rho)\right), \tag{A.21}$$

where $\mathrm{Ei}(x) = -\int_{-x}^{\infty} dt\, \frac{\mathrm{e}^{-t}}{t}$ is the exponential integral.

A.3. First order

The metric perturbation in the first order of the expansion in the beam divergence is given by [5]

$$h^{\lambda(1)}_{\alpha\beta} = \begin{pmatrix} 0 & I^{\lambda(1)}_{\xi} & I^{\lambda(1)}_{\chi} & 0 \\ I^{\lambda(1)}_{\xi} & 0 & 0 & -I^{\lambda(1)}_{\xi} \\ I^{\lambda(1)}_{\chi} & 0 & 0 & -I^{\lambda(1)}_{\chi} \\ 0 & -I^{\lambda(1)}_{\xi} & -I^{\lambda(1)}_{\chi} & 0 \end{pmatrix}, \tag{A.22}$$

where the functions $I^{\lambda(1)}_{\xi}$ and $I^{\lambda(1)}_{\chi}$ given by

$$\begin{aligned} I^{\lambda(1)}_{\xi} &= \frac{1}{4}\left(\theta\zeta\partial_{\xi} + \lambda\partial_{\chi}\right) I^{(0)} \\ &= -\frac{2GP_0w_0^2(\theta\zeta\xi + \lambda\chi)}{c^5\rho^2}\left(1 - \mathrm{e}^{-2|\mu|^2\rho^2}\right), \end{aligned} \tag{A.23}$$

$$\begin{aligned} I^{\lambda(1)}_{\chi} &= -\frac{1}{4}\left(\lambda\partial_{\xi} - \theta\zeta\partial_{\chi}\right) I^{(0)} \\ &= \frac{2GP_0w_0^2(\lambda\xi - \theta\zeta\chi)}{c^5\rho^2}\left(1 - \mathrm{e}^{-2|\mu|^2\rho^2}\right). \end{aligned} \tag{A.24}$$

A.4. Third order

The only non-zero components of the metric perturbation in the third order of the expansion in the beam divergence are given by

$$\begin{aligned} h^{\lambda(3)}_{\tau\xi} = &-\frac{GP_0w_0^2}{2c^5\rho^2}\Bigg((4\theta\zeta\xi + 3\lambda\chi) + \Bigg(-(4\theta\zeta\xi + 3\lambda\chi) - 2\rho^2(3\theta\zeta\xi + 2\lambda\chi)|\mu|^2 \\ &- 2\rho^2(-2 + 3\rho^2)(\theta\zeta\xi + \lambda\chi)|\mu|^4 + 8\rho^4(\theta\zeta\xi + \lambda\chi)|\mu|^6\Bigg)\mathrm{e}^{-2|\mu|^2\rho^2}\Bigg), \end{aligned} \tag{A.25}$$

$$h^{\lambda(3)}_{\tau\chi} = -\frac{GP_0w_0^2}{2c^5\rho^2}\Bigg((4\theta\zeta\chi - 3\lambda\xi) + \Bigg(-(4\theta\zeta\chi - 3\lambda\xi) - 2\rho^2(3\theta\zeta\chi - 2\lambda\xi)|\mu|^2 \\ - 2\rho^2(-2+3\rho^2)(\theta\zeta\chi - \lambda\xi)|\mu|^4 + 8\rho^4(\theta\zeta\chi - \lambda\xi)|\mu|^6\Bigg)\mathrm{e}^{-2|\mu|^2\rho^2}\Bigg), \tag{A.26}$$

$$h^{\lambda(3)}_{\zeta\xi} = \frac{GP_0w_0^2}{2c^5\rho^2}\Bigg((2\theta\zeta\xi + \lambda\chi) + \Bigg(-(2\theta\zeta\xi + \lambda\chi) - 2\rho^2(2\theta\zeta\xi + \lambda\chi)|\mu|^2 \\ - 2\rho^2(-2+3\rho^2)(\theta\zeta\xi + \lambda\chi)|\mu|^4 + 8\rho^4(\theta\zeta\xi + \lambda\chi)|\mu|^6\Bigg)\mathrm{e}^{-2|\mu|^2\rho^2}\Bigg), \tag{A.27}$$

$$h^{\lambda(3)}_{\zeta\chi} = \frac{GP_0w_0^2}{2c^5\rho^2}\Bigg((2\theta\zeta\chi - \lambda\xi) + \Bigg(-(2\theta\zeta\chi - \lambda\xi) - 2\rho^2(2\theta\zeta\chi - \lambda\xi)|\mu|^2 \\ - 2\rho^2(-2+3\rho^2)(\theta\zeta\chi - \lambda\xi)|\mu|^4 + 8\rho^4(\theta\zeta\chi - \lambda\xi)|\mu|^6\Bigg)\mathrm{e}^{-2|\mu|^2\rho^2}\Bigg). \tag{A.28}$$

Appendix B. Another approach to determine the rotation of polarization (as described in [11])

Another result for the rotation of the polarization was obtained in [11], where the polarization vector is parallel transported through the gravitational field, again starting and ending in flat spacetime. The angle of rotation in the $\alpha\beta$-plane is given by

$$\tilde{\Delta}_{\alpha\beta} = \int_{-\infty}^{\infty} \mathrm{d}\tilde{\tau}\ \dot{\gamma}^\gamma \Gamma^\delta_{\alpha\gamma} g_{\beta\delta}, \tag{B.1}$$

where $\tilde{\tau}$ is the parameter parametrizing the geodesic γ. It is obtained as follows: the polarization vector ω^α is parallel transported if

$$\dot{\gamma}^\alpha \partial_\alpha \omega^\gamma + \dot{\gamma}^\alpha \omega^\beta \Gamma^\gamma_{\alpha\beta} = 0. \tag{B.2}$$

Integrating along the geodesic γ, the change of polarization is given by

$$\delta\omega^\gamma = \int_{-\infty}^{\infty} \mathrm{d}\tau\ \dot{\gamma}^\alpha \partial_\alpha \omega^\gamma = -\int_{-\infty}^{\infty} \mathrm{d}\tau\ \dot{\gamma}^\alpha \omega^\beta \Gamma^\gamma_{\alpha\beta}. \tag{B.3}$$

From the change of polarization, the angle of rotation in the plane $\beta\gamma$ is obtained by writing

$$(\omega + \delta\omega)^\gamma = \left(g^\gamma{}_\beta + \tilde{\Delta}^\gamma{}_\beta\right)\omega^\beta, \tag{B.4}$$

which has the form of an infinitesimal rotation. The rotation angle is given by (B.1). This result is coordinate-invariant if the metric perturbation vanishes far away from the source of the gravitational field. This is not the case for the laser beam. However, in some cases the result can be applied, as we will explain. Also, (B.1) describes a four-dimensional rotation. If the test light-ray is deflected by the laser beam (as for the parallel counter-propagating and the transversal light ray), one has to be careful when applying this formula, as the ray-transversal plane tilts when the light ray is deflected. In our case, the formula can be applied. Indeed, it

leads to the same results as we obtain with equation (7): for the parallel co- and parallel conter-propagating light rays, one obtains (to third and first order in the expansion in θ, respectively)

$$\tilde{\Delta}^{+}_{\xi\chi} = -\frac{\theta^2}{2w_0^2}\int_{-\infty}^{\infty} \mathrm{d}(\theta\zeta)\left(\partial_\chi\left(h^{(3)}_{\xi\zeta} + h^{(3)}_{\tau\xi}\right) - \partial_\xi\left(h^{(3)}_{\chi\zeta} + h^{(3)}_{\tau\chi}\right) - \partial_{\theta\zeta}h^{(2)}_{\xi\chi}\right), \tag{B.5}$$

$$\tilde{\Delta}^{-}_{\chi\xi} = -\frac{1}{2w_0^2}\int_{-\infty}^{\infty} \mathrm{d}(\theta\zeta)\left(\partial_\chi\left(h^{(1)}_{\xi\zeta} - h^{(1)}_{\xi\tau}\right) - \partial_\xi\left(h^{(1)}_{\chi\zeta} - h^{(1)}_{\chi\tau}\right)\right). \tag{B.6}$$

The last term of the integrand in the above equation for $\tilde{\Delta}^{+}_{\xi\chi}$ vanishes when integrating from $\zeta = -\infty$ to $\zeta = \infty$, as in our case $h_{\xi\chi}(\infty) = h_{\xi\chi}(-\infty)$. Therefore, we see that $\tilde{\Delta}^{+}_{\xi\chi} = \Delta_+$ and $\tilde{\Delta}^{-}_{\chi\xi} = \Delta_-$. The same is the case for the transversally propagating light rays: we find (up to the first order in the expansion in θ)

$$\tilde{\Delta}^{t^+}_{\chi\zeta} = \frac{1}{2w_0^2}\int_{-\infty}^{\infty} \mathrm{d}\xi\left(\partial_\chi h^{(0)}_{\tau\zeta} - \theta\partial_\chi h^{(1)}_{\xi\tau} + \theta\partial_\xi h^{(1)}_{\chi\zeta}\right), \tag{B.7}$$

$$\tilde{\Delta}^{t^-}_{\zeta\chi} = \frac{1}{2w_0^2}\int_{-\infty}^{\infty} \mathrm{d}\xi\left(-\partial_\chi h^{(0)}_{\tau\zeta} - \theta\partial_\chi h^{(1)}_{\xi\tau} - \theta\partial_\xi h^{(1)}_{\chi\zeta}\right). \tag{B.8}$$

As $h^{(1)}_{\chi\zeta}(\xi = \infty) = h^{(1)}_{\chi\zeta}(\xi = -\infty)$, we obtain $\tilde{\Delta}^{t^+}_{\chi\zeta} = \Delta_{t^+}$ and $\tilde{\Delta}^{t^-}_{\zeta\chi} = \Delta_{t^-}$.

Appendix C. Derivation for finitely extended source and test beams

Starting from the solution in equation (6) for the linearized Einstein equations, we find with equation (8), using the identity $\partial_{x^a}\frac{1}{|\vec{x}-\vec{x}'|} = -\partial_{x^{a\prime}}\frac{1}{|\vec{x}-\vec{x}'|}$, and partial integration (the energy-momentum tensor vanishes at infinity)

$$\Delta_\pm = -\frac{2G}{c^4}\int_A^B \mathrm{d}\zeta\int_{-\infty}^{\infty}\mathrm{d}\xi'\mathrm{d}\chi'\mathrm{d}\zeta'\,\frac{1}{|\vec{x}-\vec{x}'|}\left(\theta\left(\partial_{\chi'}\left(t^{(1)}_{\xi\zeta} \pm t^{(1)}_{\tau\xi}\right) - \partial_{\xi'}\left(t^{(1)}_{\chi\zeta} \pm t^{(1)}_{\tau\chi}\right)\right) + \theta^3\left(\partial_{\chi'}\left(t^{(3)}_{\xi\zeta} \pm t^{(3)}_{\tau\xi}\right) - \partial_{\xi'}\left(t^{(3)}_{\chi\zeta} \pm t^{(3)}_{\tau\chi}\right)\right)\right). \tag{C.1}$$

The energy-momentum tensor of the finitely extended beam is given by multiplying the expressions in appendix A for the infinitely extended beam with the Heaviside functions $\Theta(\zeta - \alpha(\rho))$ and $\Theta(\beta(\rho) - \zeta)$, where $\alpha(\rho)$ and $\beta(\rho)$ describe the ζ-coordinate of the source beam's emitter and absorber, respectively. This truncation of the energy-momentum tensor leads to a violation of the continuity equation of general relativity, which in our case means neglecting recoil on emitter and absorber. This corresponds to energy and momentum being inserted into the system and dissipated from it, respectively, and can lead to apparent effects close to emitter and absorber that may not be present in practice. The best approximation of reality by our model of the finitely extended beam will be achieved for points far from emitter

and absorber but close to the beamline (see also [48] for a detailed analysis of a similar situation).

When the surfaces of emitter and absorber are considered to match the phase fronts of the beam, they are curved and, therefore, depend on ρ. This dependence is of second order in θ. The derivatives in equation (C.1) lead to Dirac delta functions $\alpha'(\rho)\delta(\zeta-\alpha(\rho))$ and $\beta'(\rho)\delta(\beta(\rho)-\zeta)$, and hence to evaluation of the integrand at the surfaces of emitter and absorber, respectively, integrated over the transversal directions. For each term in equation (C.1), this contributes even higher order terms. In the following, we restrict our considerations to the leading order only (to first order for Δ_- and to third order for Δ_+). Therefore, the contributions of the curved surfaces of emitter and absorber can be neglected and we set α and β to be constants. From the expressions given in appendix A for the energy-momentum tensor, one sees that $t^{(1)}_{\xi\zeta}=-t^{(1)}_{\tau\xi}$ and $t^{(1)}_{\chi\zeta}=-t^{(1)}_{\tau\chi}$. The derivatives appearing in the expression for $\Delta_\pm$ of the first order terms are given by

$$\partial_\chi t^{(1)}_{\xi\zeta}=\frac{2P_0}{\pi c}|\mu|^4\Big(-4\chi|\mu|^2(\theta\zeta\xi+\lambda\chi)+\lambda\Big)\mathrm{e}^{-2|\mu|^2\rho^2}, \tag{C.2}$$

$$\partial_\xi t^{(1)}_{\chi\zeta}=\frac{2P_0}{\pi c}|\mu|^4\Big(-4\xi|\mu|^2(\theta\zeta\chi-\lambda\xi)-\lambda\Big)\mathrm{e}^{-2|\mu|^2\rho^2}, \tag{C.3}$$

and the derivatives of the third order terms are found to be

$$\partial_\chi\Big(t^{(3)}_{\xi\zeta}+t^{(3)}_{\tau\xi}\Big)=-\frac{P_0}{\pi c}|\mu|^6\rho^2\mathrm{e}^{-2|\mu|^2\rho^2}\Big(\lambda+(-4|\mu|^2+2/\rho^2)\chi(\theta\zeta\xi+\lambda\chi)\Big), \tag{C.4}$$

$$\partial_\xi\Big(t^{(3)}_{\chi\zeta}+t^{(3)}_{\tau\chi}\Big)=-\frac{P_0}{\pi c}|\mu|^6\rho^2\mathrm{e}^{-2|\mu|^2\rho^2}\Big(-\lambda+(-4|\mu|^2+2/\rho^2)\xi(\theta\zeta\chi-\lambda\xi)\Big). \tag{C.5}$$

Considering only the leading order terms in θ, we obtain for the rotation angles of the parallel co- and the parallel counter-propagating test rays

$$\begin{aligned}\Delta_-=&-\frac{8GP_0}{c^5}\frac{2\lambda\theta}{\pi}\int_{-\infty}^{\infty}\mathrm{d}\xi'\mathrm{d}\chi'\int_\alpha^\beta\mathrm{d}\zeta' K(\xi',\chi',\zeta')\\&|\mu(\zeta')|^4(1-2|\mu(\zeta')|^2\rho'^2)\mathrm{e}^{-2|\mu(\zeta')|^2\rho'^2},\end{aligned} \tag{C.6}$$

$$\begin{aligned}\Delta_+=&\frac{8GP_0}{c^5}\frac{\lambda\theta^3}{\pi}\int_{-\infty}^{\infty}\mathrm{d}\xi'\mathrm{d}\chi'\int_\alpha^\beta\mathrm{d}\zeta' K(\xi',\chi',\zeta')\\&|\mu(\zeta')|^6\rho'^2(1-|\mu(\zeta')|^2\rho'^2)\mathrm{e}^{-2|\mu(\zeta')|^2\rho'^2},\end{aligned} \tag{C.7}$$

where $|\mu(\zeta')|^2=1/(1+(\theta\zeta')^2)$ and

$$K(\xi',\chi',\zeta')=\log\left(\frac{B-\zeta'+(\rho''^2+(B-\zeta')^2)^{1/2}}{A-\zeta'+(\rho''^2+(A-\zeta')^2)^{1/2}}\right), \tag{C.8}$$

with $\rho''=\sqrt{(\xi'-\xi)^2+(\chi-\chi')^2}$.

For the transversal test ray, we find along the same lines (neglecting again the effect of the curved surfaces of emitter and absorber as they are at least of second order in θ), using equation (D.8),

$$\Delta_{t\pm} = \frac{2G}{c^4}\int_A^B \mathrm{d}\xi \int_{-\infty}^{\infty} \mathrm{d}\xi' \mathrm{d}\chi' \mathrm{d}\zeta' \, \frac{1}{|\vec{x}-\vec{x}'|} \\ \partial_{\chi'}\left(\pm t^{(0)}_{\tau\zeta} + \theta t^{(1)}_{\xi\zeta}\right). \tag{C.9}$$

From the expressions for the energy-momentum tensor in appendix A, we find that the derivatives in the above equation are given by

$$\partial_\chi t^{(0)}_{\tau\zeta} = \frac{8P_0}{\pi c}|\mu|^4 \chi \mathrm{e}^{-2|\mu|^2\rho^2}, \tag{C.10}$$

$$\partial_\chi t^{(1)}_{\xi\zeta} = \frac{2P_0}{\pi c}|\mu|^4(\lambda(1-4|\mu|^2\chi^2) \\ - 4\theta\zeta\xi\chi|\mu|^2)\mathrm{e}^{-2|\mu|^2\rho^2} \tag{C.11}$$

which leads to the rotation angle for the transversal test ray

$$\Delta_{t\pm} = \frac{8GP_0}{c^5}\frac{1}{2\pi}\int_{-\infty}^{\infty}\mathrm{d}\xi'\mathrm{d}\chi'\int_\alpha^\beta \mathrm{d}\zeta' K_t(\xi',\chi',\zeta') \\ |\mu(\zeta')|^4\Big(\pm 4\chi' + \theta(\lambda(1-4|\mu(\zeta')|^2\chi'^2) \\ - 4\theta\zeta'\xi'\chi'|\mu(\zeta')|^2)\Big)\mathrm{e}^{-2|\mu(\zeta')|^2\rho'^2}, \tag{C.12}$$

where the function K_t is given by

$$K_t(\xi',\chi',\zeta') \\ = \log\left(\frac{B-\xi'+(\chi''^2+(\zeta-\zeta')^2+(B-\xi')^2)^{1/2}}{A-\xi'+(\chi''^2+(\zeta-\zeta')^2+(A-\xi')^2)^{1/2}}\right), \tag{C.13}$$

where $\chi'' = \chi' - \chi$.

For the numerical analysis, we transform the found expressions for the rotation angles into the cylindrical coordinates (ρ',ϕ',ζ') with $\phi' = \arccos(\xi'/\rho')$ or (ρ'',ϕ'',ζ') with $\rho'' = \sqrt{\xi'^2+\chi''^2}$ and $\phi'' = \arccos(\xi'/\rho'')$.

Appendix D. Derivation for infinitely extended source and test beams

For the parallel test rays, we obtain from equation (7) and $t_{0,\pm} = \dot{\gamma}_\pm(\tau_0) = (1,0,0,\pm(1-f^\pm))$

$$\Delta_\pm = \frac{1}{2w_0^2}\int_{-\infty}^{\infty}\mathrm{d}\tau\; t_0^a\epsilon_{abc}\partial_b h_{c\alpha}(\varrho_\perp+\tau t_0)t_0^\alpha \\ = \frac{1}{2w_0^2}\int_{-\infty}^{\infty}\mathrm{d}\tau\;\epsilon_{\zeta bc}\partial_b\left(h_{c\zeta}(\xi,\chi,\pm\tau)\pm h_{c\tau}(\xi,\chi,\pm\tau)\right) \\ = -\frac{1}{2w_0^2}\int_{-\infty}^{\infty}\mathrm{d}\zeta\;\Big(\partial_\chi(h_{\xi\zeta}\pm h_{\xi\tau}) - \partial_\xi(h_{\chi\zeta}\pm h_{\chi\tau})\Big). \tag{D.1}$$

The rotation angle for the parallel counter-propagating test ray is thus given by (considering the leading order only)

$$\Delta_- = -\frac{\theta}{2w_0^2}\int_{-\infty}^{\infty} \mathrm{d}\zeta \Big(\partial_\chi \left(h^{(1)}_{\xi\zeta} - h^{(1)}_{\tau\xi}\right) - \partial_\xi \left(h^{(1)}_{\chi\zeta} - h^{(1)}_{\tau\chi}\right)\Big). \tag{D.2}$$

From the expressions for the metric perturbation in appendix A, we see that $h^{(1)}_{\xi\zeta} = -h^{(1)}_{\tau\xi}$, $h^{(1)}_{\chi\zeta} = -h^{(1)}_{\tau\chi}$. For the derivatives in the above expression, we find

$$\partial_\chi h^{(1)}_{\xi\zeta} - \partial_\xi h^{(1)}_{\chi\zeta} = \frac{8GP_0w_0^2}{c^5}\lambda|\mu|^2 \mathrm{e}^{-2|\mu|^2\rho^2}, \tag{D.3}$$

which leads to the rotation angle for the parallel counter-propagating test ray

$$\Delta_- = -\lambda\frac{8GP_0\theta}{c^5}\int_{-\infty}^{\infty} \mathrm{d}\zeta\, |\mu|^2 \mathrm{e}^{-2|\mu|^2\rho^2}. \tag{D.4}$$

Along the same lines, we find in leading order

$$\Delta_+ = -\frac{\theta^3}{2w_0^2}\int_{-\infty}^{\infty} \mathrm{d}\zeta \left(\partial_\chi \left(h^{(3)}_{\xi\zeta} + h^{(3)}_{\tau\xi}\right) - \partial_\xi \left(h^{(3)}_{\chi\zeta} + h^{(3)}_{\tau\chi}\right)\right). \tag{D.5}$$

From the expressions for the metric perturbation in appendix A, one finds for the derivatives in the above expression

$$\partial_\chi \left(h^{(3)}_{\xi\zeta} + h^{(3)}_{\tau\xi}\right) - \partial_\xi \left(h^{(3)}_{\chi\zeta} + h^{(3)}_{\tau\chi}\right) = -\lambda\frac{2GP_0w_0^2}{c^5}|\mu|^2(1+2\rho^2|\mu|^2)\mathrm{e}^{-2|\mu|^2\rho^2}. \tag{D.6}$$

Then, the rotation angle for the parallel co-propagating light ray is given by

$$\Delta_+ = \lambda\frac{GP_0\theta^3}{c^5}\int_{-\infty}^{\infty} \mathrm{d}\zeta\, |\mu|^2(1+2\rho^2|\mu|^2)\mathrm{e}^{-2|\mu|^2\rho^2}. \tag{D.7}$$

For the transversal test ray, we obtain from equation (7) and $\dot\gamma_\pm = (1, \pm 1, 0, 0)$

$$\begin{aligned}\Delta_{t^\pm} &= \frac{1}{2w_0^2}\int_{-\infty}^{\infty} \mathrm{d}\tau\; t_0^a \epsilon_{abc}\partial_b h_{c\alpha}(\tau, \varrho_\perp + \tau t_0) t_0^\alpha \\ &= \pm\frac{1}{2w_0^2}\int_{-\infty}^{\infty} \mathrm{d}\xi\, (\partial_\chi h_{\tau\zeta} - \theta\partial_{\theta\zeta}h_{\tau\chi}) \\ &\quad + \frac{1}{2w_0^2}\int_{-\infty}^{\infty} \mathrm{d}\xi\, (\partial_\chi h_{\xi\zeta} - \theta\partial_{\theta\zeta}h_{\xi\chi})\,.\end{aligned} \tag{D.8}$$

Considering the terms up to first order in θ, it is given by

$$\Delta_{t^\pm} = \pm\frac{1}{2w_0^2}\int_{-\infty}^{\infty} \mathrm{d}\xi\, \partial_\chi h^{(0)}_{\tau\zeta} + \frac{\theta}{2w_0^2}\int_{-\infty}^{\infty} \mathrm{d}\xi\, \partial_\chi h^{(1)}_{\xi\zeta}. \tag{D.9}$$

From the expressions for the metric perturbation in appendix A, we obtain for the derivatives appearing in the above expression

$$\partial_\chi h^{(0)}_{\tau\zeta} = \frac{8GP_0w_0^2}{c^5}\frac{\chi}{\rho^2}\left(1 - \mathrm{e}^{-2|\mu|^2\rho^2}\right), \tag{D.10}$$

$$\partial_\chi h^{(1)}_{\xi\zeta} = -\frac{1}{4}(\theta\zeta\partial_\chi\partial_\xi + \lambda\partial^2_\chi)I^{(0)}. \tag{D.11}$$

The first term in equation (D.11) leads to an integration over a derivative, which vanishes,

$$\int_{-\infty}^{\infty} \mathrm{d}\xi\, \partial_\chi\partial_\xi I^{(0)} = \partial_\chi I^{(0)}\Big|_{\xi=-\infty}^{\xi=\infty} = 0. \tag{D.12}$$

Then, we obtain for the rotation angle for the transversal test ray

$$\begin{aligned}\Delta_{t^\pm} = &\pm \frac{4\pi G P_0}{c^5}\,\mathrm{erf}\left(\sqrt{2}|\mu|\chi\right)\\ &+ \lambda\frac{2\sqrt{2\pi}GP_0\theta}{c^5}\,|\mu|\mathrm{e}^{-2|\mu|^2\chi^2}.\end{aligned} \tag{D.13}$$

Appendix E. Derivation for finitely extended source beams and infinitely extended test rays

For an infinitely extended test ray and a finitely extended source beam, we obtain

$$\begin{aligned}\Delta_- = &-\frac{2G}{c^4}\partial_\chi \lim_{B\to\infty}\int_{-B}^{B}\mathrm{d}\zeta\int_{-\infty}^{\infty}\mathrm{d}\xi'\mathrm{d}\chi'\mathrm{d}\zeta'\\ &\frac{1}{|\vec{x}-\vec{x}'|}\left(t_{\xi\zeta}(\xi',\chi',\zeta') - t_{\tau\xi}(\xi',\chi',\zeta')\right)\\ &+\frac{2G}{c^4}\partial_\xi \lim_{B\to\infty}\int_{-B}^{B}\mathrm{d}\zeta\int_{-\infty}^{\infty}\mathrm{d}\xi'\mathrm{d}\chi'\mathrm{d}\zeta'\\ &\frac{1}{|\vec{x}-\vec{x}'|}\left(t_{\chi\zeta}(\xi',\chi',\zeta') - t_{\tau\chi}(\xi',\chi',\zeta')\right)\\ = &-\frac{4G\theta}{c^4}\partial_\chi\int_\alpha^\beta\mathrm{d}\zeta'\int_0^{\rho_0(\zeta')}\mathrm{d}\rho'\,\rho'\int_0^{2\pi}\mathrm{d}\phi'\\ &\lim_{B\to\infty}K_B(\xi,\chi,\zeta,\rho',\phi',\zeta')t^{(1)}_{\xi\zeta}(\rho',\phi',\zeta')\\ &+\frac{4G\theta}{c^4}\partial_\xi\int_\alpha^\beta\mathrm{d}\zeta'\int_0^{\rho_0(\zeta')}\mathrm{d}\rho'\,\rho'\int_0^{2\pi}\mathrm{d}\phi'\\ &\lim_{B\to\infty}K_B(\xi,\chi,\zeta,\rho',\phi',\zeta')t^{(1)}_{\chi\zeta}(\rho',\phi',\zeta'),\end{aligned} \tag{E.1}$$

where cylindrical coordinates $\rho' = \sqrt{\xi'^2+\chi'^2}$ and $\phi' = \arctan(\chi'/\xi')$ are used and the function K_B is given by

$$\begin{aligned}&K_B(\xi,\chi,\zeta,\rho',\phi',\zeta')\\ &= \log\left(\frac{B-\zeta'+(\rho''^2+(B-\zeta')^2)^{1/2}}{-B-\zeta'+(\rho''^2+(B+\zeta')^2)^{1/2}}\right),\end{aligned} \tag{E.2}$$

where $\rho''^2 = (\xi'-\xi)^2+(\chi'-\chi)^2 = \rho'^2+\rho^2-2\rho'\rho\cos(\phi-\phi')$, and $\rho_0(\zeta') = \rho_0/|\mu(\zeta')|$ is the finite transversal extension of the beam that is related to the width of emitter and absorber and ρ_0 is a constant. For $\beta/B \ll 1$, $-\alpha/B \ll 1$ and $\rho_0(\zeta')/B \ll 1$ for all $\zeta' \in [\alpha,\beta]$, we obtain

$$
\begin{aligned}
&K_B(\rho', \phi', \zeta') \\
&= \log\left(\frac{B - \zeta' + (\rho''^2 + B^2(1 - \zeta'/B)^2)^{1/2}}{-B - \zeta' + (\rho''^2 + B^2(1 + \zeta'/B)^2)^{1/2}}\right) \\
&\approx \log\left(\frac{2(B - \zeta') + \rho''^2/(2B(1 - \zeta'/B))}{\rho''^2/(2B(1 + \zeta'/B))}\right) \\
&= \log\left(\frac{1 + \zeta'/B}{1 - \zeta'/B} + \frac{4B^2}{\rho''^2}(1 - (\zeta'/B)^2)\right) \\
&\approx \log\left(4\frac{B^2}{\rho''^2}\right). \qquad \text{(E.3)}
\end{aligned}
$$

In order to evaluate the expression for Δ_-, one needs to take derivatives of the function K_B. One finds

$$
\begin{aligned}
&\partial_\chi \log\left(4\frac{B^2}{\rho''^2}\right) t^{(1)}_{\xi\zeta} - \partial_\xi \log\left(4\frac{B^2}{\rho''^2}\right) t^{(1)}_{\chi\zeta} \\
&= \frac{2P_0}{\pi c}|\mu'|^4 \mathrm{e}^{-2|\mu'|^2\rho''^2}\left(\lambda\rho'\partial_{\rho'} + \theta\zeta'\partial_{\phi'}\right)\log\left(\rho''^2\right). \qquad \text{(E.4)}
\end{aligned}
$$

Therefore, one finds for the following expression appearing in the expression for Δ_-,

$$
\begin{aligned}
&\partial_\chi \int_0^{\rho_0(\zeta')} \mathrm{d}\rho'\,\rho' \int_0^{2\pi} \mathrm{d}\phi' \lim_{B\to\infty} K_B(\rho', \phi', \zeta') t^{(1)}_{\xi\zeta} \\
&- \partial_\xi \int_0^{\rho_0(\zeta')} \mathrm{d}\rho'\,\rho' \int_0^{2\pi} \mathrm{d}\phi' \lim_{B\to\infty} K_B(\rho', \phi', \zeta') t^{(1)}_{\chi\zeta} \\
&= \frac{2P_0}{\pi c}|\mu'|^4 \int_0^{\rho_0(\zeta')} \mathrm{d}\rho'\,\rho' \mathrm{e}^{-2|\mu'|^2\rho''^2} \\
&\int_0^{2\pi} \mathrm{d}\phi' \left(\lambda\rho'\partial_{\rho'} + \theta\zeta'\partial_{\phi'}\right)\log\left(\rho''^2\right). \qquad \text{(E.5)}
\end{aligned}
$$

The term containing the ϕ'-derivative vanishes under the integral. With

$$
\begin{aligned}
&\rho'\partial_{\rho'} \int_0^{2\pi} \mathrm{d}\phi' \log\left(\rho''^2 + \rho^2 - 2\rho\rho'\cos(\phi' - \phi)\right) \\
&= 2\pi\rho'\partial_{\rho'} \begin{Bmatrix} \log\left(\rho''^2\right) & \text{for} & \rho \leqslant \rho' \\ \log\left(\rho^2\right) & \text{for} & \rho > \rho' \end{Bmatrix} \\
&= 4\pi \begin{Bmatrix} 1 & \text{for} & \rho \leqslant \rho' \\ 0 & \text{for} & \rho > \rho' \end{Bmatrix} = 4\pi\Theta(\rho' - \rho), \qquad \text{(E.6)}
\end{aligned}
$$

we obtain

$$\begin{aligned}
&\frac{2P_0\lambda}{\pi c}|\mu'|^4\int_0^{\rho_0(\zeta')}\mathrm{d}\rho'\,\rho'\int_0^{2\pi}\mathrm{d}\phi'\\
&\mathrm{e}^{-2|\mu'|^2\rho'^2}\rho'\partial_{\rho'}\log\left(\rho''^2\right)\\
&=-\frac{2P_0\lambda}{c}|\mu'|^2\int_0^{\rho_0(\zeta')}\mathrm{d}\rho'\,\Theta(\rho'-\rho)\partial_{\rho'}\mathrm{e}^{-2|\mu'|^2\rho'^2}\\
&=-\frac{2P_0\lambda}{c}|\mu'|^2\left\{\begin{array}{ll}\int_\rho^{\rho_0(\zeta')}\mathrm{d}\rho'\,\partial_{\rho'}\mathrm{e}^{-2|\mu'|^2\rho'^2} & :\ \rho\leqslant\rho_0(\zeta')\\ 0 & :\ \rho>\rho_0(\zeta')\end{array}\right\}\\
&=\frac{2P_0\lambda}{c}|\mu'|^2\Theta(\rho_0(\zeta')-\rho)\left(\mathrm{e}^{-2|\mu'|^2\rho^2}-\mathrm{e}^{-2|\mu'|^2\rho_0^2(\zeta')}\right).
\end{aligned}\tag{E.7}$$

Finally, we obtain for the rotation of polarization for the parallel counter-propagating test ray

$$\begin{aligned}
\Delta_-=&-\lambda\frac{8GP_0\theta}{c^5}\int_\alpha^\beta\mathrm{d}\zeta'\\
&\Theta(\rho_0-|\mu'|\rho)|\mu'|^2\left(\mathrm{e}^{-2|\mu'|^2\rho^2}-\mathrm{e}^{-2\rho_0^2}\right),
\end{aligned}\tag{E.8}$$

which leads to equation (10) for $\rho_0\to\infty$. We see that Δ_- vanishes if there is no overlap with the beam, i.e. if $\rho>\rho_0(\alpha)$ and $\rho>\rho_0(\beta)$. For large ρ, there is only an overlap for large ζ' for which $\rho_0(\zeta')\approx\rho_0\theta\zeta'$ and $|\mu'|=|\theta\zeta'|^{-1}$. Evaluating the integral, we find

$$\begin{aligned}
\Delta_-=\lambda\frac{8GP_0}{c^5\rho}\Bigg[&\Theta(-\theta\alpha-\rho/\rho_0)\left(\frac{\sqrt{\pi}}{2\sqrt{2}}\left(\mathrm{erf}\left(-\frac{\sqrt{2}\rho}{\theta\alpha}\right)-\mathrm{erf}\left(\sqrt{2}\rho_0\right)\right)-\mathrm{e}^{-2\rho_0^2}\left(-\frac{\rho}{\theta\alpha}-\rho_0\right)\right)\\
&+\Theta(\theta\beta-\rho/\rho_0)\left(\frac{\sqrt{\pi}}{2\sqrt{2}}\left(\mathrm{erf}\left(\frac{\sqrt{2}\rho}{\theta\beta}\right)-\mathrm{erf}\left(\sqrt{2}\rho_0\right)\right)-\mathrm{e}^{-2\rho_0^2}\left(\frac{\rho}{\theta\beta}-\rho_0\right)\right)\Bigg].
\end{aligned}\tag{E.9}$$

For $\rho_0\to\infty$, we obtain

$$\begin{aligned}
\Delta_-=&-\lambda\frac{4GP_0}{c^5\rho}\frac{\sqrt{\pi}}{\sqrt{2}}\\
&\left(\mathrm{erfc}\left(\frac{\sqrt{2}\rho}{\theta\beta}\right)+\mathrm{erfc}\left(\frac{\sqrt{2}\rho}{\theta|\alpha|}\right)\right),
\end{aligned}\tag{E.10}$$

where erfc is the complementary error function. For $\rho\gg\theta\beta$ and $\rho\gg-\theta\alpha$, using the asymptotic expansion of the complementary error function, we obtain

$$\Delta_-\approx-\lambda\frac{2GP_0\theta}{c^5\rho^2}\left(\beta\mathrm{e}^{-2(\rho/\theta\beta)^2}+|\alpha|\mathrm{e}^{-2(\rho/\theta\alpha)^2}\right).\tag{E.11}$$

For Δ_+, it follows from equation (C.1) that in leading order (third order in θ), the rotation of polarization for the parallel co-propagating light ray is given by

$$
\begin{aligned}
\Delta_+ = & -\frac{2G}{c^4}\partial_\chi \lim_{B\to\infty}\int_{-B}^{B}\mathrm{d}\zeta \\
& \int_{-\infty}^{\infty}\mathrm{d}\xi'\mathrm{d}\chi'\mathrm{d}\zeta'\,\frac{1}{|\vec{x}-\vec{x}'|}\left(t_{\xi\zeta}+t_{\tau\xi}\right) \\
& +\frac{2G}{c^4}\partial_\xi \lim_{B\to\infty}\int_{-B}^{B}\mathrm{d}\zeta \\
& \int_{-\infty}^{\infty}\mathrm{d}\xi'\mathrm{d}\chi'\mathrm{d}\zeta'\,\frac{1}{|\vec{x}-\vec{x}'|}\left(t_{\chi\zeta}+t_{\tau\chi}\right) \\
= & -\frac{2G\theta^3}{c^4}\partial_\chi\int_\alpha^\beta\mathrm{d}\zeta'\int_0^{\rho_0(\zeta')}\mathrm{d}\rho'\,\rho' \\
& \int_0^{2\pi}\mathrm{d}\phi'\,\lim_{B\to\infty}K_B(\rho',\phi',\zeta')\left(t^{(3)}_{\xi\zeta}+t^{(3)}_{\tau\xi}\right) \\
& +\frac{2G\theta^3}{c^4}\partial_\xi\int_\alpha^\beta\mathrm{d}\zeta'\int_0^{\rho_0(\zeta')}\mathrm{d}\rho'\,\rho' \\
& \int_0^{2\pi}\mathrm{d}\phi'\,\lim_{B\to\infty}K_B(\rho',\phi',\zeta')\left(t^{(3)}_{\xi\zeta}+t^{(3)}_{\tau\xi}\right). \qquad \text{(E.12)}
\end{aligned}
$$

The relevant combination of derivatives of the function K_B with the approximation given in equation (E.3) is given by

$$
\begin{aligned}
& \partial_\chi\log\left(4\frac{B^2}{\rho''^2}\right)\left(t^{(3)}_{\xi\zeta}+t^{(3)}_{\tau\xi}\right) \\
& -\partial_\xi\log\left(4\frac{B^2}{\rho''^2}\right)\left(t^{(3)}_{\chi\zeta}+t^{(3)}_{\tau\chi}\right) \\
& =-\frac{P_0}{\pi c}|\mu'|^6\rho'^2\mathrm{e}^{-2|\mu'|^2\rho'^2}\left(\lambda\rho'\partial_{\rho'}+\theta\zeta'\partial_{\phi'}\right)\log\left(\rho''^2\right). \qquad \text{(E.13)}
\end{aligned}
$$

Again, the term containing the derivative with respect to ϕ' vanishes under the integration over ϕ' and we obtain

$$
\begin{aligned}
& -\frac{P_0\lambda}{\pi c}|\mu'|^6\int_0^{\rho_0(\zeta')}\mathrm{d}\rho'\,\rho'^3\int_0^{2\pi}\mathrm{d}\phi' \\
& \mathrm{e}^{-2|\mu'|^2\rho'^2}\rho'\partial_{\rho'}\log\left(\rho''^2\right) \\
& =\frac{P_0\lambda}{c}|\mu'|^4\int_0^{\rho_0(\zeta')}\mathrm{d}\rho'\,\Theta(\rho'-\rho)\rho'^2\partial_{\rho'}\mathrm{e}^{-2|\mu'|^2\rho'^2} \\
& =\frac{P_0\lambda}{c}|\mu'|^4\begin{Bmatrix}\int_\rho^{\rho_0(\zeta')}\mathrm{d}\rho'\,\rho'^2\partial_{\rho'}\mathrm{e}^{-2|\mu'|^2\rho'^2} & : \rho\leqslant\rho_0(\zeta') \\ 0 & : \rho>\rho_0(\zeta')\end{Bmatrix}
\end{aligned}
$$

$$
\begin{aligned}
&= -\frac{P_0\lambda}{c}|\mu'|^4\Theta(\rho_0(\zeta')-\rho)\Bigg[2\int_{\rho}^{\rho_0(\zeta')}\mathrm{d}\rho'\,\rho'\mathrm{e}^{-2|\mu'|^2\rho'^2}\\
&\quad+\left(\rho^2\mathrm{e}^{-2|\mu'|^2\rho^2}-\rho_0(\zeta')^2\mathrm{e}^{-2|\mu'|^2\rho_0(\zeta')^2}\right)\Bigg]\\
&= -\frac{P_0\lambda}{c}|\mu'|^2\Theta(\rho_0(\zeta')-\rho)\Bigg[-\frac{1}{2}\int_{\rho}^{\rho_0(\zeta')}\mathrm{d}\rho'\,\partial_{\rho'}\mathrm{e}^{-2|\mu'|^2\rho'^2}\\
&\quad+|\mu'|^2\left(\rho^2\mathrm{e}^{-2|\mu'|^2\rho^2}-\rho_0(\zeta')^2\mathrm{e}^{-2|\mu'|^2\rho_0(\zeta')^2}\right)\Bigg]\\
&= -\frac{P_0\lambda}{2c}|\mu'|^2\Theta(\rho_0(\zeta')-\rho)\Big((1+2|\mu'|^2\rho^2)\mathrm{e}^{-2|\mu'|^2\rho^2}\\
&\quad-(1+2|\mu'|^2\rho_0(\zeta')^2)\mathrm{e}^{-2|\mu'|^2\rho_0(\zeta')^2}\Big).
\end{aligned}
\tag{E.14}
$$

Finally, the rotation of polarization for the parallel co-propagating light ray is given by

$$
\begin{aligned}
\Delta_+ &= \lambda\frac{GP_0\theta^3}{c^5}\int_{\alpha}^{\beta}\mathrm{d}\zeta'\\
&\quad\Theta(\rho_0-|\mu'|\rho)|\mu'|^2\Big((1+2|\mu'|^2\rho^2)\mathrm{e}^{-2|\mu'|^2\rho^2}\\
&\quad-(1+2\rho_0^2)\mathrm{e}^{-2\rho_0^2}\Big),
\end{aligned}
\tag{E.15}
$$

which leads to equation (9) for $\rho_0\to\infty$. In this case, we find that

$$
\Delta_+ = -\frac{\theta^2}{8}\Big(1-\partial_\sigma\Big)\Delta_-(\sqrt{\sigma}\rho)\Big|_{\sigma=1}.
\tag{E.16}
$$

Again, we find that Δ_+ vanishes if there is no overlap with the beam, i.e. if $\rho>\rho_0(\alpha)$ and $\rho>\rho_0(\beta)$. For $\rho_0\to\infty$, $\rho\gg\theta\beta$ and $\rho\gg-\theta\alpha$, we find

$$
\begin{aligned}
\Delta_+ &= \lambda\frac{GP_0\theta^3}{2c^5}\left(\beta\left(\frac{1}{\rho^2}+\frac{1}{(\theta\beta)^2}\right)\mathrm{e}^{-2(\rho/\theta\beta)^2}\right.\\
&\quad\left.-\alpha\left(\frac{1}{\rho^2}+\frac{1}{(\theta\alpha)^2}\right)\mathrm{e}^{-2(\rho/\theta\alpha)^2}\right)\\
&\approx \lambda\frac{GP_0\theta}{2c^5}\left(\frac{1}{\beta}\mathrm{e}^{-2(\rho/\theta\beta)^2}+\frac{1}{|\alpha|}\mathrm{e}^{-2(\rho/\theta\alpha)^2}\right).
\end{aligned}
\tag{E.17}
$$

For $\Delta_{t^\pm}$ for a finitely extended source beam and an infinitely extended test ray we obtain, considering only the leading order contribution,

$$
\begin{aligned}
\Delta^{(0)}_{t^\pm} &= \pm\frac{1}{2w_0^2}\int_{-\infty}^{\infty}\mathrm{d}\xi\,\partial_\chi h^{(0)}_{\tau\zeta}\\
&= \mp\frac{2G}{c^4}\int_{\alpha}^{\beta}\mathrm{d}\zeta'\int_{\rho\leqslant\rho_0(\zeta')}\mathrm{d}\xi'\mathrm{d}\chi'\\
&\quad\lim_{B\to\infty}\partial_\chi K_{t,B}(\xi',\chi',\zeta')t^{(0)}_{\tau\zeta},
\end{aligned}
\tag{E.18}
$$

where the function $K_{t,B}$ is given by

$$K_{t,B}(\xi',\chi',\zeta') = \log\left(\frac{B-\xi'+(\chi''^2+(\zeta-\zeta')^2+(B-\xi')^2)^{1/2}}{-B-\xi'+(\chi''^2+(\zeta-\zeta')^2+(B+\xi')^2)^{1/2}}\right), \tag{E.19}$$

and where $\chi''=\chi'-\chi$. For $B\gg 1$, we obtain

$$\begin{aligned}
&K_{t,B}(\xi',\chi',\zeta')\\
&= \log\left(\frac{B-\xi'+(B-\xi')\Big(1+(\chi''^2+(\zeta-\zeta')^2)/(B-\xi')^2\Big)^{1/2}}{-B-\xi'+(B+\xi')\Big(1+(\chi''^2+(\zeta-\zeta')^2)/(B+\xi')^2\Big)^{1/2}}\right)\\
&\approx \log\left(\frac{B-\xi'+(B-\xi')\Big(1+(\chi''^2+(\zeta-\zeta')^2)/(2(B-\xi')^2)\Big)}{-B-\xi'+(B+\xi')\Big(1+(\chi''^2+(\zeta-\zeta')^2)/(2(B+\xi')^2)\Big)}\right)\\
&= \log\left(\frac{2(B-\xi')+(\chi''^2+(\zeta-\zeta')^2)/(2(B-\xi'))}{(\chi''^2+(\zeta-\zeta')^2)/(2(B+\xi'))}\right)\\
&\approx \log\left(\frac{B+\xi'}{B-\xi'}+\frac{4B^2}{\chi''^2+(\zeta-\zeta')^2}(1-\xi'^2/B^2)\right)\\
&\approx \log\left(\frac{4B^2}{\chi''^2+(\zeta-\zeta')^2}\right).
\end{aligned} \tag{E.20}$$

With the derivative of $K_{t,B}$ with respect to χ,

$$\partial_\chi \log\left(\frac{4B^2}{\chi''^2+(\zeta-\zeta')^2}\right) = 2\frac{\chi-\chi'}{\chi''^2+(\zeta-\zeta')^2} \tag{E.21}$$

we obtain for the zeroth order of the rotation of polarization of the transversal test ray

$$\begin{aligned}
\Delta_{t^\pm}^{(0)} = \mp\frac{4GP_0}{\pi c^5}\int_\alpha^\beta \mathrm{d}\zeta' \int_{\rho\leqslant\rho_0(\zeta')} \mathrm{d}\xi'\mathrm{d}\chi'\\
\frac{\chi-\chi'}{\chi''^2+(\zeta-\zeta')^2}|\mu'|^2\mathrm{e}^{-2|\mu'|^2\rho'^2}.
\end{aligned} \tag{E.22}$$

Note that for $\chi=0$, the integrand is anti-symmetric in χ' and $\Delta_{t^\pm}^{(0)}$ vanishes. For the first order contribution, we find

$$\begin{aligned}
\Delta_{t^\pm}^{(1)} = \lambda\frac{4GP_0}{\pi c^5}\int_\alpha^\beta \mathrm{d}\zeta' \int_{\rho\leqslant\rho_0(\zeta')} \mathrm{d}\xi'\mathrm{d}\chi'\\
\frac{\chi'(\chi-\chi')}{(\chi-\chi')^2+(\zeta-\zeta')^2}|\mu'|^4\mathrm{e}^{-2|\mu'|^2\rho'^2}.
\end{aligned} \tag{E.23}$$

For $\chi=0$, the integrand is symmetric in χ' and $\Delta_{t^\pm}^{(1)}$ does not vanish.

Appendix F. Multipole expansion of the far field for finitely extended source and test beams

For the finitely extended source beam, one can get analytical approximations of Δ in the far field. For simplicity we assume here that the source beam extends from $-\beta$ to β, and the probe beam from $-B$ to B. The maximal radial extension of the source beam, reached at $\zeta' = \pm\beta$, is then given by $\rho' = \theta\beta/\sqrt{2}$. This is the maximum scale on which all components of the energy-stress tensor and its derivatives fall off like a Gaussian (for smaller values of $|\zeta'|$ the decay is even faster). Far field means then that the probe beam should be a distance $\rho \gg \theta\beta/\sqrt{2}$ from the source beam when passing parallel to the source beam. A much shorter distance of order $\rho \simeq 1$ suffices for the transversal beam passing at the beam waist for being in the far field regime.

From equations (6) and (8) we obtain, after shifting derivatives to the prime-coordinates and partial integration,

$$\begin{aligned}\Delta_{\pm} = &-\frac{2G}{c^4\theta}\int_{-B}^{B} \mathrm{d}(\theta\zeta)\int \mathrm{d}^3x' \frac{1}{|\vec{x}-\vec{x}'|}\\ &\Big[\partial_{\chi'}(T_{\xi\zeta}(\vec{x}') \pm T_{\tau\xi}(\vec{x}'))\\ &-\partial_{\xi'}(T_{\chi\zeta}(\vec{x}') \pm T_{\tau\chi}(\vec{x}'))\Big].\end{aligned} \tag{F.1}$$

For the partial integration we assume once more that we are in the far-field, so that boundary terms are exponentially suppressed through the Gaussian factor $\exp(-2|\mu|^2\rho^2)$. The source term relevant for Δ_- is given to first order in θ by (see appendix A, equations (A.22)

$$\begin{aligned}S_-(\rho',\zeta') &\equiv \frac{\pi c}{4P_0\theta}\Big[\partial_{\chi'}(T_{\xi\zeta}(\vec{x}') - T_{\tau\xi}(\vec{x}'))\\ &\qquad -\partial_{\xi'}(T_{\chi\zeta}(\vec{x}') - T_{\tau\chi}(\vec{x}'))\Big]\\ &= \frac{2\mathrm{e}^{-2\frac{\rho'^2}{1+\theta^2\zeta'^2}}\lambda(1+\theta^2\zeta'^2-2\rho'^2)}{(1+\theta^2\zeta'^2)^3}.\end{aligned} \tag{F.2}$$

Manifestly, S_- enjoys azimuthal symmetry. It is then useful to expand the function $1/|\vec{x}-\vec{x}'|$ as (see e.g. [49] p 93)

$$\frac{1}{|\vec{x}-\vec{x}'|} = \sum_{l=0}^{\infty}\frac{r_<^l}{r_>^{l+1}}P_l(\cos\vartheta')P_l(\cos\vartheta)\,, \tag{F.3}$$

where P_l are the Legendre-polynomials, $r_<$ ($r_>$) is the smaller (larger) of $|\vec{x}|$ and $|\vec{x}'|$, and ϑ (ϑ') the angle between the z-axis and $\vec{x}$ ($\vec{x}'$). For calculating the far field, we can set everywhere $r_> = r = |\vec{x}|$ and $r_< = r' = |\vec{x}'|$. This leads to

$$\begin{aligned}\Delta_- &= \sum_{l=0}^{\infty}\Delta_-^{(l)}\\ &= -\frac{16GP_0\theta}{c^5}\sum_{l=0}^{\infty}\int_{-B}^{B}\mathrm{d}\zeta\frac{Q_-^{(l)}}{(\rho^2+\zeta^2)^{(l+1)/2}}P_l\left(\frac{\zeta}{\sqrt{\rho^2+\zeta^2}}\right),\end{aligned} \tag{F.4}$$

where the multipoles $Q_-^{(l)}$ are given by

$$Q_-^{(l)} = \int_{-\beta}^{\beta} \mathrm{d}\zeta' \int_0^{\infty} \rho' \mathrm{d}\rho' \, (\rho'^2 + \zeta'^2)^{l/2} \times P_l\left(\frac{\zeta'}{\sqrt{\rho'^2 + \zeta'^2}}\right) S_-(\rho', \zeta'), \tag{F.5}$$

and we have used that in cylinder coordinates $\vartheta = \arccos(\zeta/\sqrt{\rho^2 + \zeta^2})$, and correspondingly for ϑ'. The multipoles and their contributions to Δ_- can be calculated analytically. All odd multipoles vanish, and so do the monopole and dipole contribution ($l = 0, 1$, respectively). Δ_- is then dominated by the quadropole contribution $l = 2$. The correction due to higher order multipoles $l = 4, 6, ...$ decays quickly with l. We therefore limit ourselves to listing the results for $l = 2, 4, 6$. Note that the direct dependence on ζ' of $1/|\vec{x} - \vec{x}'|$ (rather than on $\theta\zeta$ as for the rest of the integrand) brings about additional θ dependence. Neglecting these higher order terms, we find

$$Q_-^{(2)} = \frac{\beta\lambda}{4}, \tag{F.6}$$

$$Q_-^{(4)} = \frac{\beta\lambda}{8}(-3 + 4\beta^2), \tag{F.7}$$

$$Q_-^{(6)} = \frac{3\beta\lambda}{64}(15 - 40\beta^2 + 16\beta^4), \tag{F.8}$$

and, with $\Omega \equiv 8\lambda\theta G P_0/c^5$,

$$\Delta_-^{(2)} = \frac{\Omega\beta}{2} \frac{B}{(B^2 + \rho^2)^{3/2}}, \tag{F.9}$$

$$\Delta_-^{(4)} = \frac{\Omega\beta(-3 + 4\beta^2)}{16} \frac{(2B^3 - 3B\rho^2)}{(B^2 + \rho^2)^{7/2}}, \tag{F.10}$$

$$\Delta_-^{(6)} = \frac{\Omega\beta(15 - 40\beta^2 + 16\beta^4)}{256} \frac{(8B^4 - 40B^2\rho^2 + 15\rho^4)}{(B^2 + \rho^2)^{11/2}}. \tag{F.11}$$

For Δ_+, the lowest contributing terms are from the derivatives of the third order of the metric. The expression for S_- is replaced by S_+ given by

$$\begin{aligned} S_+(\rho', \zeta') &\equiv \frac{\pi c}{P_0\theta^2}\Big[\partial_{\chi'}(T_{\xi\zeta}(\vec{x}') + T_{\tau\xi}(\vec{x}')) \\ &\quad - \partial_{\xi'}(T_{\chi\zeta}(\vec{x}') + T_{\tau\chi}(\vec{x}'))\Big] \\ &= -\frac{\mathrm{e}^{-2\frac{\rho'^2}{1+\theta^2\zeta'^2}} \lambda\rho'^2(1 - \rho'^2/(1 + \theta^2\zeta'^2))}{(1 + \theta^2\zeta'^2)^3}. \end{aligned} \tag{F.12}$$

Also here the monopole contribution ($l = 0$) and all contributions with odd l, in particular the dipole contribution ($l = 1$) vanish. The lowest order non-vanishing contributions are

$$Q_+^{(2)} = -\frac{\beta\lambda\theta^2}{16}, \tag{F.13}$$

$$Q_+^{(4)} = \frac{\beta\lambda\theta^2}{64}(9 - 8\beta^2), \tag{F.14}$$

$$Q_+^{(6)} = -\frac{3\beta\lambda\theta^2}{128}(15 - 30\beta^2 + 8\beta^4), \tag{F.15}$$

to be substituted into the expression corresponding to (F.4), i.e.

$$\begin{aligned}\Delta_+ &= \sum_{l=0}^{\infty} \Delta_+^{(l)} \\ &= -\frac{16GP_0\theta}{c^5} \sum_{l=0}^{\infty} \int_{-B}^{B} \mathrm{d}\zeta \frac{Q_+^{(l)}}{(\rho^2+\zeta^2)^{(l+1)/2}} P_l\left(\frac{\zeta}{\sqrt{\rho^2+\zeta^2}}\right).\end{aligned} \tag{F.16}$$

This leads to

$$\Delta_+^{(2)} = -\frac{\Omega\theta^2}{8}\frac{B\beta}{(B^2+\rho^2)^{3/2}}, \tag{F.17}$$

$$\Delta_+^{(4)} = \frac{\Omega\theta^2(-9+8\beta^2)}{128}\frac{(-2B^3+3B\rho^2)}{(B^2+\rho^2)^{7/2}}, \tag{F.18}$$

$$\begin{aligned}\Delta_+^{(6)} = &-\frac{\Omega\theta^2 B\beta(15-30\beta^2+8\beta^4)}{512} \\ &\frac{(8B^4-40B^2\rho^2+15\rho^4)}{(B^2+\rho^2)^{11/2}},\end{aligned} \tag{F.19}$$

where we recall that Ω contains already one factor θ. So both $\Delta_\pm$ fall off as $1/\rho^3$ in the far-field due to the quadrupole contribution. For fixed ρ, β that contribution decays as $1/B$ for large B, i.e. $B \gg \rho$. This can be traced back to the integral over ζ in and would not be the case for the monopole contribution.

For $\Delta_{t^\pm}$ we start with the lowest, zeroth order in θ. It is then useful to keep the derivatives of the energy-stress tensor outside the calculation of the multipoles, as otherwise the cylindrical symmetry gets spoiled. We find

$$\Delta_{t^\pm}^{(0)} = \mp\frac{8GP_0}{c^5}\int_{-B}^{B}\mathrm{d}\xi\,\partial_\chi \sum_{l=0}^{\infty}\frac{P_l\left(\frac{\zeta}{\sqrt{\rho^2+\zeta^2}}\right)}{(\rho^2+\zeta^2)^{(l+1)/2}} Q_{t^\pm}^{(0)(l)}, \tag{F.20}$$

$$\begin{aligned}Q_{t^\pm}^{(0)(l)} = &\int_{-\beta}^{\beta}\mathrm{d}\zeta'\int_0^{\infty}\mathrm{d}\rho'\rho'(\rho'^2+\zeta'^2)^{l/2}P_l\left(\frac{\zeta'}{\sqrt{\rho'^2+\zeta'^2}}\right) \\ &\times\frac{1}{1+\theta^2\zeta'^2}\mathrm{e}^{-2\frac{\rho'^2}{1+\theta^2\zeta'^2}}.\end{aligned} \tag{F.21}$$

Also here, all the odd-power multipoles ($l = 1, 3, 5, \ldots$) vanish due to the fact that the Legendre-polynomials of odd order are odd, whereas the rest of the integrand in $Q_{t^\pm}^{(0)(l)}$ is even in ζ'. The three lowest non-vanishing multipoles read

$$Q_{t^\pm}^{(0)(0)} = \frac{\beta}{2}, \tag{F.22}$$

$$Q_{t^\pm}^{(0)(2)} = -\frac{1}{24}\beta(3-4\beta^2), \tag{F.23}$$

$$Q_{t^\pm}^{(0)(4)} = \frac{1}{160}\beta(15-40\beta^2+16\beta^4). \tag{F.24}$$

The corresponding contributions to $\Delta_{t^\pm}$ at $\zeta = 0$ are

$$\Delta_{t^\pm}^{(0)(0)} = \pm\tilde{\Omega}\frac{B\beta}{\chi\sqrt{B^2+\chi^2}}, \tag{F.25}$$

$$\Delta_{t^\pm}^{(0)(2)} = \pm\tilde{\Omega}\frac{B\beta(3-4\beta^2)(2B^2+3\chi^2)}{24\chi^3(B^2+\chi^2)^{3/2}}, \tag{F.26}$$

$$\Delta_{t^\pm}^{(0)(4)} = \pm\tilde{\Omega}\frac{B\beta(15-40\beta^2+16\beta^4)}{640\chi^5(B^2+\chi^2)^{5/2}} (8B^4+20B^2\chi^2+15\chi^4), \tag{F.27}$$

where $\tilde{\Omega} = 8GP_0/c^5$. We see that now there is a contribution from the monopole that leads to a decay as $1/\chi^2$ with the minimal distance χ from the beamline when evaluated at $\zeta = 0$ and in the limit of $\chi \gg B$. The next (quadrupole) term contributes a $1/\chi^4$ decay. In the limit of $B \to \infty$ at fixed χ, the monopole contribution converges to a β/χ^2 behavior.

For the first order term in $\Delta_{t^\pm}$, the contribution to the Faraday effect, we obtain with the expressions for the energy-momentum tensor given in appendix A, using the symmetry of $|\vec{x}-\vec{x}'|$ and performing a partial integration,

$$\begin{aligned}\Delta_{t^\pm}^{(1)} &= \frac{2G\theta}{c^4}\partial_\chi\int_{-B}^{B}\mathrm{d}\xi\int_{-\infty}^{\infty}\mathrm{d}\xi'\mathrm{d}\chi'\mathrm{d}\zeta'\,\frac{1}{|\vec{x}-\vec{x}'|}t_{\xi\zeta}^{(1)}\\ &= \frac{\lambda\theta}{4}\partial_\chi\Delta_{t^+}^{(0)} - \frac{GP_0\theta^2}{\pi c^5}\partial_\chi\int_{-B}^{B}\mathrm{d}\xi\,\partial_\xi\int_{-\infty}^{\infty}\mathrm{d}\xi'\mathrm{d}\chi'\\ &\quad\int_{-\beta}^{\beta}\mathrm{d}\zeta'\frac{1}{|\vec{x}-\vec{x}'|}\frac{\zeta'}{1+\theta^2\zeta'^2}\mathrm{e}^{-2\frac{\rho'^2}{1+\theta^2\zeta'^2}}.\end{aligned} \tag{F.28}$$

We neglect the second term as it is of higher order in θ. For the first term, we find from the multipole expansion of $\Delta_{t^+}^{(0)}$ for $\zeta = 0$

$$\Delta_{t^\pm}^{(1)(0)} = -\frac{\lambda\theta}{4}\tilde{\Omega}\frac{B\beta(B^2+2\chi^2)}{\chi^2(B^2+\chi^2)^{3/2}}, \tag{F.29}$$

$$\Delta_{t^\pm}^{(1)(2)} = -\frac{\lambda\theta}{4}\tilde{\Omega}\frac{B\beta(3-4\beta^2)}{8\chi^4(B^2+\chi^2)^{5/2}} (2B^4+5B^2\chi^2+4\chi^4), \tag{F.30}$$

$$\Delta_{t^\pm}^{(1)(4)} = -\frac{\lambda\theta}{4}\tilde{\Omega}\frac{B\beta(15-40\beta^2+16\beta^4)}{128\chi^6(B^2+\chi^2)^{7/2}} (8B^6+28B^4\chi^2+35B^2\chi^4+18\chi^6). \tag{F.31}$$

In a real experiment, it should be kept in mind that the gravitational effects from emitter and absorber and the power-supplies feeding them, as well as heat-radiation from the absorber may lead to effects that mask the rotation of the polarization of the source beam itself in the far field, if their dipole- or monopole-contributions do not vanish. If one wishes to evaluate these effects, a careful modelling of the entire setup will be necessary.

Appendix G. The infinitely thin beam

The metric perturbation induced by an infinitely thin beam of light that extends along the ζ-axis from $-\beta$ to β is given by the only non-zero components $h_{\tau\tau} = -h_{\tau\zeta} = h_{\zeta\zeta} = h$, where h is given as [1]

$$h = \frac{4GP_0w_0^2}{c^5}\log\left(\frac{\beta-\zeta+(\rho^2+(\beta-\zeta)^2)^{1/2}}{-\beta-\zeta+(\rho^2+(\beta+\zeta)^2)^{1/2}}\right). \tag{G.1}$$

Therefore, we find with equation (7) at $\zeta = 0$ and for large χ

$$\begin{aligned}\Delta_{t^\pm} &\approx \pm\frac{1}{2w_0^2}\int_{-B}^{B} \mathrm{d}\xi\, \partial_\chi h^{(0)}_{\tau\zeta}\\ &\approx \pm\frac{8GP_0}{c^5}\frac{\beta B}{\chi\sqrt{B^2+\chi^2}},\end{aligned} \tag{G.2}$$

where we considered a test ray extending from $-B$ to B, and

$$\Delta_{t^\pm} \approx \pm\frac{8GP_0}{c^5}\frac{\beta}{\chi}, \tag{G.3}$$

for the infinitely extended test ray.

ORCID iDs

Dennis Rätzel https://orcid.org/0000-0003-3452-6222
Daniel Braun https://orcid.org/0000-0001-8598-2039

References

[1] Tolman R C, Ehrenfest P and Podolsky B 1931 On the gravitational field produced by light *Phys. Rev.* **37**
[2] Bonnor W B 1969 The gravitational field of light *Commun. Math. Phys.* **13** 163–74
[3] Rätzel D, Wilkens M and Menzel R 2016 Gravitational properties of light—the gravitational field of a laser pulse *New J. Phys.* **18** 023009
[4] Strohaber J 2018 General relativistic manifestations of orbital angular and intrinsic hyperbolic momentum in electromagnetic radiation (arXiv:1807.00933)
[5] Schneiter F, Rätzel D and Braun D 2018 The gravitational field of a laser beam beyond the short wavelength approximation *Class. Quantum Grav.* **35** 195007
[6] Skrotskii G V 1957 The influence of gravity on the propagation of light *Dokl. Akad. Nauk SSSR* **114** 73–6
[7] Balazs N L 1958 Effect of a gravitational field, due to a rotating body, on the plane of polarization of an electromagnetic wave *Phys. Rev.* **110** 236
[8] Plebanski J 1960 Electromagnetic waves in gravitational fields *Phys. Rev.* **118** 1396–408
[9] Lyutikov M 2017 Rotation of polarization by a moving gravitational lens *Phys. Rev.* D **95** 124003

[10] Kopeikin S and Mashoon B 2002 Gravitomagnetic effects in the propagation of electromeagnetic waves in variable gravitational fields of arbitrary-moving and spinning bodies *Phys. Rev.* D **65** 064025
[11] Pen U-L, Wang X and Yang I-S 2017 Gravitational rotation of polarization: clarifying the gauge dependence and prediction for a double pulsar *Phys. Rev.* D **95** 044034
[12] Sereno M 2004 Gravitational Faraday rotation in a weak gravitational field *Phys. Rev.* D **69** 087501
[13] Chen B 2015 Probing the gravitational Faraday rotation using quasar x-ray microlensing *Sci. Rep.* **5** 16860
[14] Piran T and Safier P N 1985 A gravitational analogue of Faraday rotation *Nature* **318** 271–3
[15] Dehnen H 1973 Gravitational Faraday-effect *Int. J. Theor. Phys.* **7** 467–74
[16] Cox D E, O'Brien J G, Mallett R L and Roychoudhuri C 2007 Gravitational Faraday effect produced by a ring laser *Found. Phys.* **37** 723–33
[17] Ji P and Bai Y 2006 Gravitational effects induced by high-power lasers *Eur. Phys. J.* C **46** 817–23
[18] Gnedin N Y and Dymnikova I G 1988 Rotation of the plane of polarization of a photon in a Petrov type $\mathcal{D}$ space-time *Zh. Eksp. Teor. Fiz.* **94** 26–31
[19] Brodutch A, Demarie T F and Terno D R 2011 Photon polarization and geometric phase in general relativity *Phys. Rev.* D **84** 104043
[20] Brodutch A and Terno D R 2011 Polarization rotation, reference frames and Mach's principle *Phys. Rev.* D **84** 121501
[21] Landau L and Lifschitz E M 1974 *Lehrbuch der Theoretischen Physik, Band VIII, Elektrodynamik der Kontinua (German edition)* 3rd edn (Berlin: Akademie)
[22] Calkin M G 1965 An invariance property of the free electromagnetic field *Am. J. Phys.* **33** 958–60
[23] Trueba J L and Rañada A F 1996 The electromagnetic helicity *Eur. J. Phys.* **17** 141
[24] Barnett S M, Cameron R P and Yao A M 2012 Duplex symmetry and its relation to the conservation of optical helicity *Phys. Rev.* A **86** 013845
[25] Fernandez-Corbaton I, Zambrana-Puyalto X and Molina-Terriza G 2012 Helicity and angular momentum: a symmetry-based framework for the study of light-matter interactions *Phys. Rev.* A **86** 042103
[26] Andersson L, Aghapour S and Bhattacharyya R 2018 Helicity and spin conservation in Maxwell theory and linearized gravity (arXiv:1812.03292)
[27] Misner C W, Thorne K S and Wheeler J A 1973 *Gravitation* (San Francisco, CA: W. H. Freeman and Company)
[28] Levi-Civita T 1919 *Atti Accad. Lincei Rendi* **28**
[29] Rätzel D, Schneiter F, Braun D, Bravo T, Howl R, Lock M P E and Fuentes I 2018 Frequency spectrum of an optical resonator in a curved spacetime *New J. Phys.* **20** 053046
[30] Aichelburg P C and Sexl R U 1971 On the gravitational field of a massless particle *Gen. Relativ. Gravit.* **2** 303–12
[31] Braun D, Schneiter F and Fischer U R 2017 Intrinsic measurement errors for the speed of light in vacuum *Class. Quantum Grav.* **34** 175009
[32] Leonhardt U and Philbin T G 2006 General relativity in electrical engineering *New J. Phys.* **8** 247
[33] Valle F D, Milotti E, Ejlli A, Gastaldi U, Messineo G, Piemontese L, Zavattini G, Pengo R and Ruoso G 2014 Extremely long decay time optical cavity *Opt. Express* **22** 11570
[34] Schottky W 1918 Über spontane Stromschwankungen in verschiedenen Elektrizitätsleitern *Ann. Phys., Lpz.* **57** 541–67
[35] Shcherbakov E A, Fomin V V, Abramov A A, Ferin A A, Mochalov D V and Gaspontsev V P 2013 Industrial grade 100 kW power CW fiber laser *Advanced Solid-State Lasers Congress* ed G Huber and P Moulton (Washington, DC: Optical Society of America) p ATh4A.2
[36] Meng L S, Brasseur J K and Neumann D K 2005 Damage threshold and surface distortion measurement for high-reflectance, low-loss mirrors to 100 + MW cm^{-2} CW laser intensity *Opt. Express* **13** 10085–91
[37] Vahlbruch H, Mehmet M, Danzmann K and Schnabel R 2016 Detection of 15 db squeezed states of light and their application for the absolute calibration of photoelectric quantum efficiency *Phys. Rev. Lett.* **117** 110801
[38] Pinel O, Jian P, Treps N, Fabre C and Braun D 2013 Quantum parameter estimation using general single-mode Gaussian states *Phys. Rev.* A **88** 040102
[39] Braun D, Adesso G, Benatti F, Floreanini R, Marzolino U, Mitchell M W and Pirandola S 2018 Quantum-enhanced measurements without entanglement *Rev. Mod. Phys.* **90** 035006

[40] Aasi J *et al* 2013 Enhanced sensitivity of the LIGO gravitational wave detector by using squeezed states of light *Nat. Photon.* **7** 613–9
[41] Faraoni V 1993 On the rotation of polarization by a gravitational lens *J. Astrophys. Astron.* **272** 385–8
[42] Kobzarev I Y and Selivanov K G 1988 Rotation of the polarization vector in a nonstationary gravitational field *Zh. Eksp. Teor. Fiz.* **94** 1–4
[43] van Holten J W 2011 The gravitational field of a light wave *Fortschr. Phys.* **59** 284–95
[44] Barker B M, Bhatia M S and Gupta S N 1967 Gravitational scattering of light by light *Phys. Rev.* **158** 1498
[45] Mashhoon B 2000 Gravitational couplings of intrinsic spin *Class. Quantum Grav.* **17** 2399
[46] Strohaber J 2013 Frame dragging with optical vortices *Gen. Relativ. Gravit.* **45** 2457–65
[47] Mallett R L 2000 Weak gravitational field of the electromagnetic radiation in a ring laser *Phys. Lett.* A **269** 214–7
[48] Rätzel D, Wilkens M and Menzel R 2016 The effect of entanglement in gravitational photon–photon scattering *Europhys. Lett.* **115** 51002
[49] Jackson J D 1999 *Classical Electrodynamics* 3rd edn (New York: Wiley)